DEPARTMENT OF ELECTRICAL AND COMPUTER ENGINEERING

TECHNICAL UNIVERSITY OF MUNICH

Bachelor's Thesis in Electrical and Computer Engineering

Eye Blink Detection and Motor Imagery Using A Wireless EEG: An Investigation

Karahan Yilmazer

DEPARTMENT OF ELECTRICAL AND COMPUTER ENGINEERING

TECHNICAL UNIVERSITY OF MUNICH

Bachelor's Thesis in Electrical and Computer Engineering

Eye Blink Detection and Motor Imagery Using A Wireless EEG: An Investigation

Author:	Karahan Yilmazer
Supervisor:	Prof. Dr. Gordon Cheng
Advisor:	Nicolas Berberich
Submission Date:	17.01.2022

I confirm that this bachelor's thesis in electrical and computer engineering is my own work and I have documented all sources and material used.

Munich, 17.01.2022 Karahan Yilmazer

Acknowledgments

It is my pleasure to thank everyone who helped and guided me throughout the writing of this dissertation.

First and foremost, I would like to thank my supervisor Prof. Dr. Gordon Cheng, for his guidance and support. His previous work was a vital source of motivation for me.

In addition, I am grateful for the support and assistance of my advisor Nicolas Berberich. His broad knowledge of the field has made it possible for me to see possible approaches to the problem at hand. When I felt stuck, his guidance was of utmost importance to me.

I want to thank my colleagues Onur İçin and Mohamad Issa for the lively discussions and their great support. Furthermore, I would like to thank Patrick Hinz, An Binh Vu, Jin Ho Lee, Po-Chuan Chan, and Natalia Paredes for their valuable feedback and for motivating me with my work.

The Institute for Cognitive Systems at the Technical University of Munich provided all the necessary equipment for my work. I am grateful for this opportunity.

Lastly, I would like to thank my family and friends who always showed interest in my work.

Abstract

In this study, a single frontal channel from an 8-channel wireless dry electrode EEG system was used to design a system that can reliably detect single and double eye blinks. This system was then evaluated based on its reaction time and detection accuracy with different feedback conditions. It was shown that within one session, participants could wirelessly control the peripherals of an ESP32 microcontroller using their blinks.

In the second part of the study a publicly available motor imagery data set acquired with a 59 channel EEG was analyzed using event-related desynchronization/synchronization (ERD/ERS) curves, common spatial patterns (CSP), and sparse filter band common spatial patterns (SFBCSP). With these methods, classification accuracies of above 90% could be achieved.

The last part consisted of recording and analyzing motor imagery data using the same EEG system used for the eye blink detection system. Finally, the results were analyzed to investigate whether the designed eye blink detection system can be used to aid motor imagery brain-computer interfaces.

Contents

1 Introduction

Humans can interface with computers in manifold ways. Moving a mouse to control a cursor on a computer screen, using voice recognition systems, and touching screens to navigate smartphones can be named as some of the most prominent examples. These interfaces are so embedded in daily life that new designs mainly focus on making them faster, more accurate, and robust. However, another possibility to consider is to design new ways of interfacing.

The question may arise whether this is needed. Current interfaces seem to be working well for healthy and capable people. Nevertheless, there is no need to be conservative to change. When the interfaces used daily were first introduced, they were also novelties. So, there is always room for improvement.

Furthermore, the most popular interfaces can be unusable in some specific cases, especially for patients with neurological conditions. Some of them cannot move their hands to touch screens or use voice recognition software for extended periods because they may run out of breath. It is of utmost importance that interfaces get developed that are useful for such patients to have less dependency on others and more control in their lives.

These considerations led to systems that bypass most motor functions and communicate directly with the brain. Such a system is generally defined as a brain-computer interface (BCI). One of the leading fields in BCI research is the use of electroencephalogram (EEG). Using an EEG-based BCI, it is theoretically possible to help humans interface with machines more efficiently.

One of many such possibilities is to use the motor imagery (MI) paradigm. It has been the most researched EEG-based BCI paradigm for a long time [1]. This accumulated knowledge makes MI an excellent candidate for investigating the use of such BCIs for reliable human-computer interfacing.

The main problem of MI-BCIs is that it requires extensive training. Concretely, users may need several training sessions to learn how to operate a MI BCI [2]. This need for extensive training raises the question of whether other control signals can aid MI-BCIs by increasing their degrees of freedom and allowing faster results, for example, being able to use EEG to control external devices within one session.

For this purpose, a control signal had to be used that can be easily detected by EEG. As discussed in more detail in the upcoming chapters, EEG is prone to undesired noise, usually referred to as "artifacts" in the BCI terminology. Since these artifacts are so prominent in EEG recordings, one idea is to use them as control signals. Although this seems unintuitive at first, it was shown that non-neural artifacts cause a small impact on MI-BCI performance. Especially ocular artifacts alone had no significant influence,

probably because they affect a lower frequency band than the one of interest for MI [3]. Previous work also showed that horizontal eye movements could be combined with ERDs caused by MI [4]. Thus, it became interesting whether eye blinks can be reliably detected using EEG and whether this system could support multiple control signals.

Two systems were designed to answer these questions. The first system can detect single blinks, whereas the second can detect both single and double blinks. These systems had to be tested for accuracy and speed to investigate whether they could be used in real-life situations, e.g., for smart home assistance. This application would already be particularly helpful for patients with neurological conditions.

After successfully building and testing the proposed eye blink detector systems, whether an MI-BCI could be built with the Unicorn Hybrid Black by g.tec medical engineering GmbH, an 8-channeled dry electrode EEG used for this study, had to be investigated.

As a starting point, it was studied whether the methods proposed in previous studies like event-related desynchronization/synchronization (ERD/ERS), common spatial patterns (CSP), and sparse filter band common spatial patterns (SFBCSP) could be used to distinguish between different MI classes. For this purpose, first, a data set provided by the Berlin BCI group for the BCI Competition IV (data set 1) was analyzed [5]. Then the same methods were applied to a data set that was recorded for this study using Unicorn Hybrid Black following the paradigm to record the data set 2b from again the BCI Competition IV. This data set was provided by the Graz University of Technology [6]. Again, all these were done to investigate whether the wireless EEG system consisting of eight dry electrodes used for this study could extend the eye blink detection system with MI.

This study shows that eye blinks can be reliably used as control outputs for, e.g., home assistance systems. Tested participants could control the system and acquire high accuracy rates within only one session. This study also demonstrates how previously designed methods perform for analyzing the Berlin BCI data set and a data set recorded with Unicorn Hybrid Black following the paradigm used for the Graz data set.

The following questions give an overview of the research questions addressed by this study:

1. Can single eye blinks be detected using a single EEG channel? How does this system perform?
2. Can double eye blinks be detected using a single EEG channel? How does this system perform?
3. Can the eye blink detection system be reliably used within only one session?
4. Does feedback influence the eye blink detection system?
5. Can the detected blinks be used as control signals for IoT (Internet of Things) devices?

6. How do offline analysis methods perform on an "ideal" data set?
7. How do offline analysis methods perform on a data set recorded with the Unicorn Hybrid Black?
8. Can an online MI-BCI be realized with the Unicorn Hybrid Black?
9. Can the eye blink detection system be extended to support MI?

2 Scientific Background and Related Research

2.1 EEG

At the time of writing EEG is the most widely used method of recording brain activity [7]. It mostly consists of an elastic cap with holes inside for circular electrodes, also referred to as channels. These electrodes can be active or passive. Active electrodes amplify the EEG signal at the electrode, whereas for passive electrodes, this is done externally.

Depending on whether a conductive electrolyte gel is applied to the electrodes, the EEG system can be wet or dry. This gel lowers the impedance value of the electrodes and this results in a minimization of the noise in the data. High frequency 50 Hz line noise or slow drifts coming from the skin potential can thus be minimized. So, wet EEG systems come with the advantage of better signal quality, but it also takes time to apply the gel to each electrode. Furthermore, the participant being recorded has to wash their hair after the recording is over. This makes wet EEG systems a good candidate for research but not for real-life applications, for example, in a home setting.

On the other hand, dry electrode systems can be mounted very quickly without the need for applying gel to each electrode. The signal quality of such systems is more questionable than wet electrode systems and highly depends on the system. Dry electrode systems mostly do not offer impedance measurements, so the researcher is mostly left with the output signal to make a decision whether the signal quality is good enough for the recording.

EEG data has high temporal but poor spatial resolution [8]. This is mostly because recorded EEG dynamics is exclusively large scale and independent of electrode size [9]. The way electrodes play a role, however, is the spatial coverage. It is only intuitive to put as many sensors as possible to an area of interest. For example, if motor imagery is being researched, one would want to populate the somatosensory area (see Figure 2.1) with many electrodes.

2.1.1 EEG Recording Artifacts

While recording brain activities, it is mostly the case that signals from irrelevant sources get picked up by the recording system. These undesired signals are referred to as noise or artifacts, and EEG is notoriously susceptible to them. A wide range of sources can cause artifacts. Common artifacts for EEG recordings are the high frequency line noise

(50 or 60 Hz depending on where the recording is done), muscle activity, skin potential drifts, movement of the participant, electromagnetic interference coming from other electronic devices, and eye blinks.

Since there is a big variety of noise sources, researchers have also been working on ways to remove these noise sources from recordings. This is mostly done by spatial and temporal filtering methods that can increase the signal-to-noise ratio (SNR) by enhancing the control signal and/or reducing noise [10]. But one thing to keep in mind is that a cleaned signal cannot replace a clean signal.

2.2 Motor Imagery

EEG recordings are well-suited to capturing oscillatory brain activity or "brain waves" [8]. These brain waves are generated by the synchronous activity of large neuron populations and have characteristic frequency ranges and spatial distributions. One of such brain waves is called "alpha waves" or "alpha rhythm" and falls in the range of 8-13 Hz. It is a very dominant brain wave that can even be seen in EEG recordings without the need for extensive filtering.

A brain wave of interest for this study is the mu rhythm that oscillates with a frequency of 8-12 Hz. As it can be seen, the alpha and mu rhythm frequency bands overlap. The difference is, however, their spatial distributions. While the alpha rhythm is mostly observed in the occipital region, the mu rhythm is seen over the sensorimotor region (see Figure 2.1). Thus it is also referred to as the sensorimotor rhythm. Actually sensorimotor rhythms fall into two more major frequency bands: beta (18-30) and gamma (30-200+ Hz) [11]. But due to the Nyquist Theorem, to be able to reliably capture the whole Gamma rhythm, sampling rates over 500 have to be used. So most researchers focus on the mu and the beta bands. For the purpose of this study, the main focus will be on the mu band.

It was repeatedly shown that there is a decrease in the mu rhythm during limb movement [12] [13] [14]. This decrease is called the event-related desynchronization (ERD) [15]. If however the SMRs are increased in association with sensorimotor rhythms, it is called a event-related synchronization (ERS) [16]. Interestingly the ERDs are observed also when a movement is imagined. This is called a motor imagery (MI). It is the act of imagining a motion but not executing it.

It was shown that MI produced neural activity that is spatiotemporally similar to the motor execution case but smaller in magnitude [17]. The main focus of this study is the MI of the hands. The MI imagery of the hands cause an ERD for the contralateral and an ERS for the ipsilateral hemisphere [8]. In simpler terms, this means that right hand MI causes an ERD on the left hemisphere while a left hand MI causes an ERD of the right hemisphere. Looking at the electrode positions on a typical EEG setup, it can be concluded that during a left hand MI an ERD has to be seen at the C4 electrode, whereas a right hand MI should cause an ERD at the C3 electrode. The corresponding plots can be seen in 2.3a.

This phenomenon is also captured by the so called motor homunculus seen in Figure 2.1 (b). The homunculus is a geometric mapping between body parts and motor/somatosensory cortex and it again shows that the hands are contralaterally arranged.

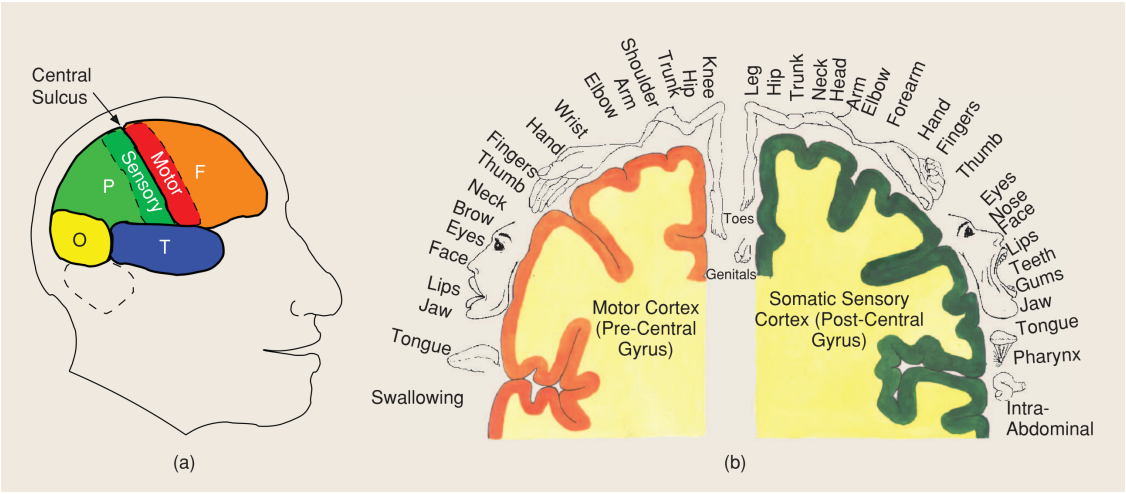

Source: Blankertz - Optimizing Spatial filters for Robust EEG Single-Trial Analysis [18]
Figure 2.1: (a) Lobes of the brain: frontal, parietal, occipital, and temporal (named after the bones of the skull beneath which they are located). The central sulcus separates the frontal and parietal lobe. (b) Geometric mapping between body parts and motor/somatosensory cortex. The motor cortex and the somatosensory cortex are shown at the left and right part of the figure, respectively. Note that in each hemisphere there is one motor area (frontal to the central sulcus) and one sensori area (posterior to the central sulcus). The part which is not shown can be obtained by mirroring the figure folded at the center. [18]

2.3 ERD/ERS Calculation

The classical ERD/ERS method calculates the instantaneous power as:

$$\overline{P}_j = \frac{1}{N}\sum_{i=1}^{N} x_{f_{i,j}}^2 \tag{2.1}$$

where $\overline{P}_j$ is the averaged power estimation of band-pass filtered data (averaged over all trials) and $x_{f_{i,j}}$ is the j-th sample of the i-th trial of the band-pass filtered data [19].

This estimation of the band power is then divided into the period of interest A and the baseline or reference period R. Consecutively, the ERD or ERS is defined as [20]:

$$ERD_j = \frac{A_j - R}{R} \cdot 100\% \tag{2.2}$$

with

$$R = \frac{1}{k} \sum_{j=n_0}^{n_0+k} A_j \tag{2.3}$$

where A_j is the power at the j-th sample.
A schematic showing the steps of this method can be found in Figure 2.2

2.4 Spatial Filtering

As the name suggests, spatial filtering is filtering signals in the spatial domain. This means that the positional relationships of the signals are taken into account. In the case of EEG recordings, this mostly refers to the positions of the electrodes. Possible goals of spatial filtering include increasing the SNR, enhancing local activity, identifying hidden sources, or finding projections that maximize discrimination between classes [8].

2.4.1 Re-referencing

A commonly used spatial filtering method is re-referencing. Three main re-referencing methods are bipolar, Laplacian, and common average referencing (CAR). An overview of these methods can be found in Figure 2.4 and two of them will be introduced below.

2.4.1.1 Surface Laplacian

There are two different surface Laplacians, namely the small Laplacian and the large Laplacian. The small Laplacian is obtained by re-referencing an electrode to the mean of its four direct neighbors. Whereas for the large Laplacian the next nearest neighbors are used.

The Laplacian method acts as a high-pass spatial filter that makes localized activity more prominent and reduces more spread out activity. Simulation studies showed that it can achieve high spatial resolution given that there is enough sensor coverage, e.g., 64 channels [10]. But it was shown that good results can be obtained from only nine channels [22]. It has to be noted that border electrodes are omitted during Laplacian re-referencing [23].

2.4.1.2 Common Average Reference

Common average reference is quite similar to the Laplacian method as it also acts as a high-pass spatial filter. This time all available channels are used to compute the mean and this mean is used as the new reference. In other words, the average over all electrodes is subtracted from each electrode. The idea is that this averaged brain activity

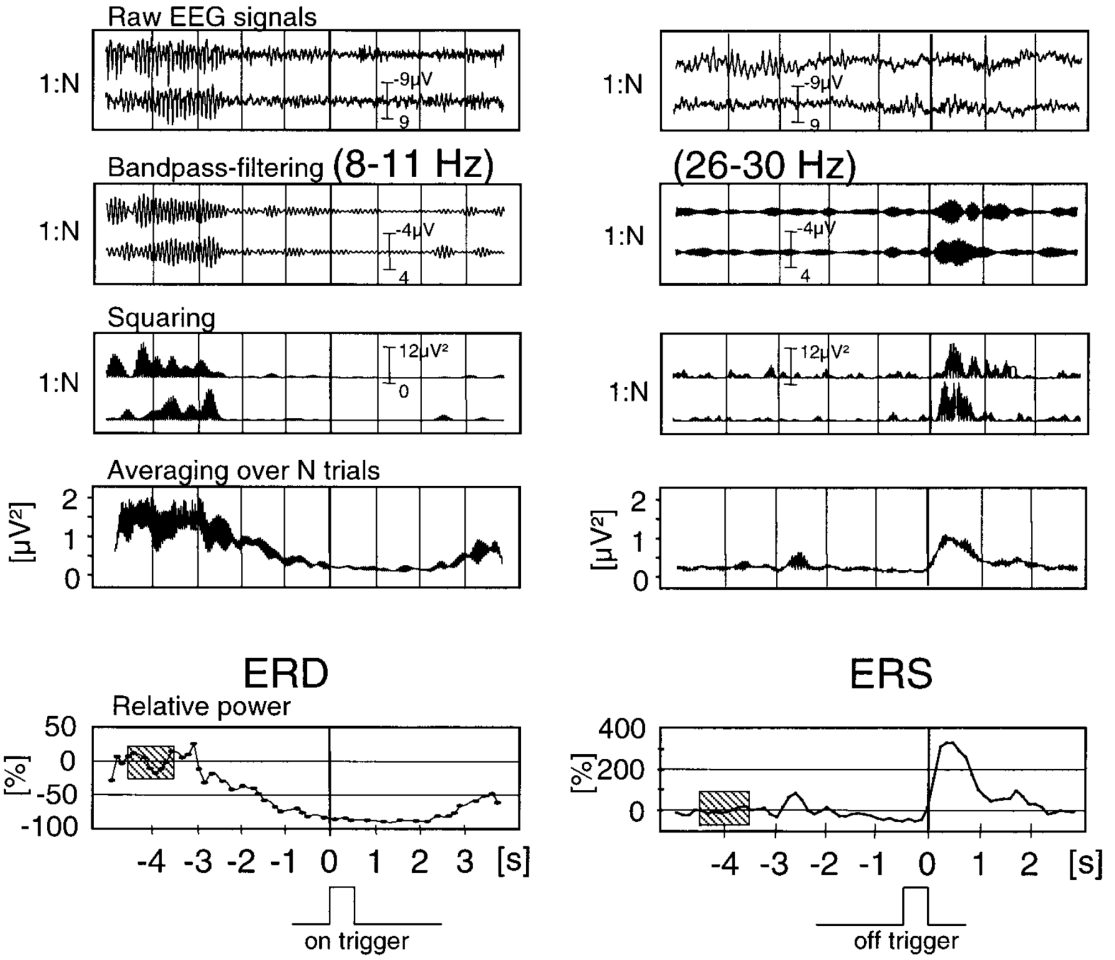

Source: Pfurtscheller and Lopes da Silva - Event-related EEG/MEG synchronization and desynchronization: Basic principles [20]

Figure 2.2: Schematic diagram showing the computation steps of ERD/ERS. The raw EEG data is first band-pass filtered in the frequency range of interest. Then the filtered signal is squared and averaged over each trial. On the left plot an ERD can be seen, that is recognizable by the decrease in the relative power. The right plot shows an increase in the band power, which is referred to as an ERS.

is the EEG noise [24]. As the same operation is done on each electrode, CAR does not privilege any particular electrode [25] and this can be easily seen from its equation:

$$\tilde{s_i} = s_i - \frac{1}{N}\sum_{n=1}^{N} s_i \tag{2.4}$$

where s_i is the signal from channel i and $\tilde{s_i}$ is the re-referenced signal.

2.4.2 Common Spatial Patterns

As mentioned before, the band powers play a very important role when it comes to designing BCIs. Bearing in mind that a convenient way to get an estimate of band powers of filtered EEG signals is to compute their variance [23], it becomes clear that an efficient algorithm that can discriminate different types of brain activity shall rely on the variances of filtered data. Given that the labels of filtered data variances are known, common spatial patterns (CSP) can be used for this purpose.

CSP is a supervised spatial filtering method that transforms EEG data into a new space where the variance of one class is maximized whereas the variance of the other class is minimized [26]. Consequently two classes can be discriminated more easily. Later work showed that it can also be extended to be used in a multi-class setting [27].

CSP was first introduced in [28]. Then it was first used in EEG analysis to extract abnormal components from the clinical EEG [29]. CSP was later adapted to EEG data classification of movement-related patterns [30]. Now, it is a widely used method to classify EEG data, especially motor imagery.

In most studies a wide filter band is used. This band can vary from 8-30 Hz [23] to 4-40 Hz [31] depending on the application. The argumentation behind this choice is that this broad frequency band contains both the mu and beta frequency bands which were shown to be important for movement classification [32]. In one study it was shown that the 8-30 Hz broad band outperformed narrow bands in classification [30].

Although the implementation can vary slightly based on the study, it is going to be introduced in the following as it was used in this study:

The first step is to band-pass filter the data in the range of interest, in accordance with the previous discussion about the frequency band. The filtered continuous data is then epoched. This means that it is cut into individual trials or epochs. Each epoch is usually time-locked to a cue, for example the start of a motor imagery period during the recording.

Let it be assumed that raw EEG data for a single epoch is represented as an NxT matrix X, where N is the number of channels and T is the number of samples per channel in each epoch. Trivially T is dependent on the sampling rate of the EEG system and the epoching window.

Due to the band-pass filtering, the constant part of the EEG data has been removed and the mean of the distribution is thus zero. That is why the first place to look for

characteristic information is in its second moments, or the covariance matrix [30]. The normalized spatial covariance matrix of the EEG can then be estimated as:

$$R = \frac{XX^T}{trace(XX^T)} \tag{2.5}$$

The matrix products correspond to averaging over time [30] and the trace normalization is done to eliminate magnitude variations in the EEG among different individuals [29]. It has to be noted that this normalization can be omitted. In this case the covariance matrix is estimated as XX^T.

The covariance matrix is then computed for both classes separately:

$$R_1 = \frac{X_1X_1^T}{trace(X_1X_1^T)}$$

$$R_2 = \frac{X_2X_2^T}{trace(X_2X_2^T)}$$

where the subscripts denote different classes (e.g. left and right hand imagery).

The next step is the eigenvalue decomposition of the composite covariance matrix which is the sum of the covariance matrices computed earlier:

$$R_c = R_1 + R_2$$

$$R_c = U\lambda U^T \tag{2.6}$$

Since R_c is a real symmetric matrix, U is an NxN orthogonal matrix whose columns are orthonormal eigenvectors of R_c and λ is a diagonal matrix whose entries are the corresponding eigenvalues.

The whitening transformation is then defined as:

$$P = \lambda^{-1/2}U^T \tag{2.7}$$

This transformation equalizes the variances in the space spanned by the eigenvectors in U [30]. If the class-specific covariance matrices are transformed using this whitening matrix by

$$S_1 = PR_1P^T \tag{2.8}$$

$$S_2 = PR_2P^T \tag{2.9}$$

then S_1 and S_2 share common eigenvectors (basic spatial patterns), since

$$S_1 + S_2 = PR_cP^T = I$$

If the eigenvalue decomposition of S_1 is given as

$$S_1 = B\psi_1 B^T \tag{2.10}$$

then the S_2 can be factored as:

$$S_2 = B\psi_2 B^T \tag{2.11}$$

where B is orthonormal.

In this case the diagonal eigenvalue matrices ψ_1 and ψ_2 always add up to the identity matrix:

$$\psi_1 + \psi_2 = I \tag{2.12}$$

Thus the variance accounted for by the first m eigenvectors which correspond to the m largest eigenvalues in ψ_1 will be maximal for class 1. Due to the constraint on ψ_2 in equation 2.12, the variances accounted for by these eigenvectors must be minimal for class 2. The reverse will hold true for the last m eigenvectors [29].

The CSP projection matrix is calculated as:

$$W_{CSP} = B^T P \tag{2.13}$$

Finally, the CSP projection matrix can be computed as:

$$Z = W_{CSP}^T X \tag{2.14}$$

The columns of of W_{CSP}^{-1} are the so called common spatial patterns and can be seen as time-invariant EEG source distribution vectors.

The feature vector can be calculated as:

$$g_p = log(\frac{var(Z_p)}{\sum_{p=1}^{2m} var(Z_p)}) \tag{2.15}$$

To calculate the feature vector, the first and last m rows of Z are used. a common value for m is 2 [30]. Conversely g_p[1] has the length $2m$. This vector can be computed for each trial and then concatenated into a feature matrix F:

$$G = [g_1, g_2, ..., g_{2m}]^T \tag{2.16}$$

[1] In the literature the feature vector is usually denoted by f_p. Here g_p was used for notation instead to avoid confusion with the frequency sub-bands from SFBCSP.

2.4.3 Sparse Filter Band Common Spatial Patterns

CSP has been proven to produce very good results when it comes to EEG data classification [30] [33] [34] [18]. But a major setback is the participant-specific filter bands to give to the CSP algorithm. It is very difficult to determine this individual frequency bands for each application, as it would require extensive searching. Furthermore, as discussed before, a poor selection of the filter band may result in poor performance of the CSP [35] [18]. This is why various different approaches were proposed to boost the effectiveness of CSP.

Common sparse spectral spatial patterns (CSSSP) aims to find spectral patterns which are common across channels by optimizing an adaptive finite impulse response (FIR) filter simultaneously with the CSP [36].

On the other hand, an intuitive solution to the individual-specific optimal frequency bands problem is to compute the CSP of different frequency sub-bands and combining the results in an efficient manner. Thus, sub-band common spatial patterns (SBCSP) proposes to do exactly this. SBCSP filters the EEG data at different frequency sub-bands and computes the CSP for each of these sub-bands. Linear discriminant analysis (LDA) is then used to decrease the dimensionality of the feature matrix [37].

Similar to this approach is the sparse filter band common spatial patterns (SFBCSP). This method uses sparse regression to automatically choose the significant CSP features computed from individual sub-bands [31].

For SFBCSP, raw EEG data is band-pass filtered using a set of overlapping subbands. The sub-bands are chosen from the frequency range 4-40 Hz with a bandwidth of 4 Hz and an overlapping rate of 2 Hz. This means K=17 sub-bands are extracted: fb_1 = 4-8 Hz, fb_1 = 6-10 Hz, ..., fb_K = 36-40 Hz.

The next step is to compute the CSP features of each sub-band using equation 2.15. This results in a feature matrix G:

$$G = \begin{bmatrix} g_{1,1} & \cdots & g_{1,2MK} \\ \vdots & \ddots & \vdots \\ g_{N,1} & \cdots & g_{N,2MK} \end{bmatrix} \tag{2.17}$$

Here, $g_{i,j}$ denotes the j-th features extracted from i-th epoch. $N = N_1 + N_2$ is the total number of epochs which is calculated by summing the number of epochs for both classes.

SFBCSP then uses the Lasso estimate [38] for significant CSP feature selection:

$$u = \arg\min_{u} \frac{1}{2} \|Gu - y\|_2^2 + \lambda \|u\|_1 \tag{2.18}$$

where $\|.\|_1$ denotes the l_1-norm, y the vector containing class labels, and u the sparse feature vector to be learned based on the sparsity vector λ. A larger λ could result in a more sparse u and the optimal value is chosen by cross-validation.

After learning is done, the non-zero coefficients of u are the significant features to be used. Since the ordering of the feature vector is equal to the ordering of the columns

of G, after learning is done, the results can be visualized for each participant to show which frequency sub-bands are optimal for them. Exemplary results from the original study can be found in Figure 2.5. It can be seen that the chosen sub-bands for each participant is different, which is in line with the previously mentioned phenomenon that the optimal frequency bands for CSP are usually participant-specific.

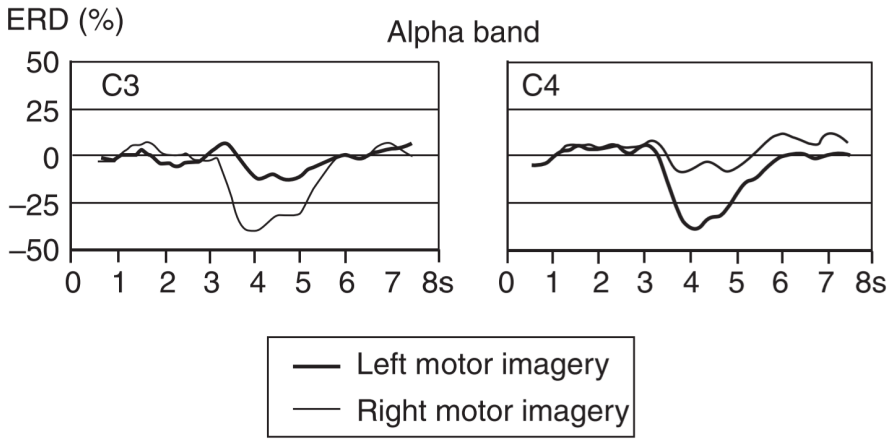

Source: Pfurtscheller et al. - Current Trends in Graz Brain–Computer Interface (BCI) Research [21]

(a) Average power in the alpha band (here, 9–13 Hz; called the mu band over motor areas) during motor imagery based on EEG signals from the left (C3) and right sensorimotor cortex (C4). Positive and negative deflections, with respect to baseline (0.5 to 2.5 seconds), represent a band power increase (ERS) and decrease (ERD) respectively. The cue was presented at 3s for 1.25 seconds. [8]

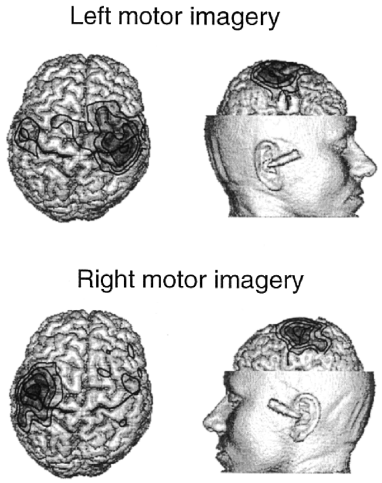

Source: Pfurtscheller et al. - Current Trends in Graz Brain–Computer Interface (BCI) Research [21]

(b) Distribution of ERD on the cortical surface calculated from a realistic head model, shown 625 ms after presentation of the cue [8]

Figure 2.3: Oscillatory EEG activity used in the Graz BCI.

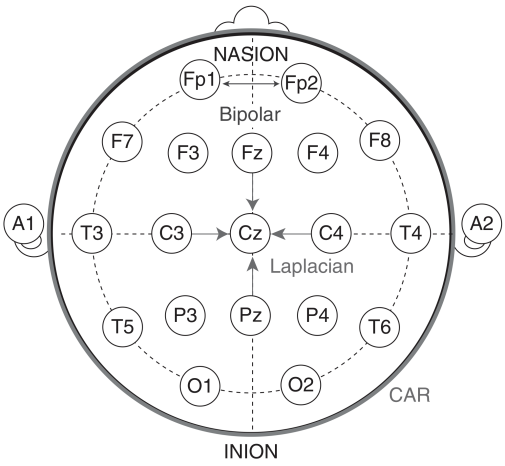

Source: Rao, Brain-Computer Interfacing: An Introduction. [8]

Figure 2.4: Schematic diagram showing three basic spatial filtering techniques. Bipolar filtering involves taking the difference between two electrodes. Laplacian filtering involves subtracting from each electrode the average of four nearest- neighbor electrodes. Common average referencing (CAR; outer circle) involves subtracting the average over all electrodes.

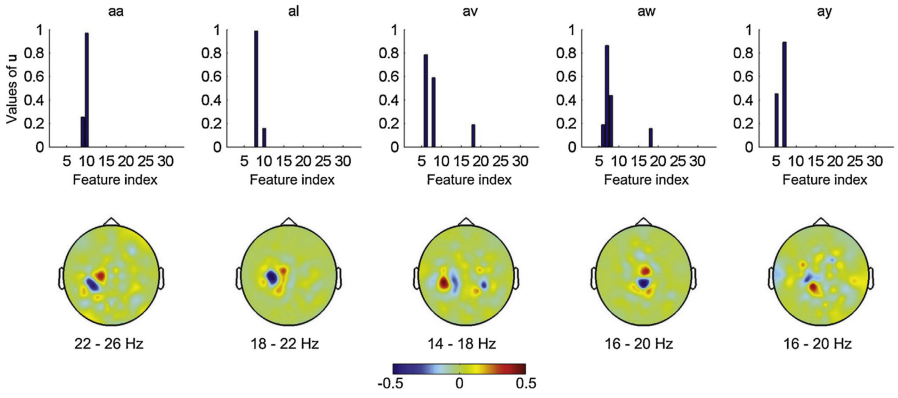

Source: Zhang et al., Optimizing spatial patterns with sparse filter bands for motor-imagery based brain–computer interface [31]

Figure 2.5: Sparse vectors and the most significant spatial filters learned by the SFBCSP method for each of the five participants in BCI Competition III dataset IVa. The feature indicated as 1, 2, ..., 34 correspond to the filter subbands 4-8 Hz, 6-10 Hz, ..., 36-40 Hz respectively.

3 Experimentation and Evaluation

3.1 Design of the Experiments

3.1.1 Setting Up the EEG

The experimentation for the eye blink detection was done with a wireless EEG system by g.tec neurotechnology GmbH called Unicorn Hybrid Black (UHB). UHB is a wireless EEG system that comes with a Bluetooth 2.1 interface. It also has a 3-axis (x, y, z) accelerometer and a gyroscope to detect head movements.

UHB consists of eight conductive rubber electrodes (Fz, C3, Cz, C4, Pz, PO7, Oz, PO8) with 24 bits resolution, a sampling rate of 250 Hz per channel, and an input sensitivity of $\pm$ 750 mV. The electrodes can be used for both dry or wet measurements (with conductive gel). A picture of the system and its sensor coverage can be seen in Figure 3.1.

For the purpose of this study, only dry measurements were made as the developed systems were intended to be used for home assistance. It has to be kept in mind that it is generally not feasible to use a wet electrode system for such an application due to the extra effort and time to set up the system, as discussed before. Especially when it comes to patients with neurological conditions, this becomes even more unfeasible.

Before putting on the EEG cap on the participant's head, two sticky reference electrodes were placed behind the ears on the mastoids. Then the distance between the nasion and inion was measured. After mounting the EEG cap, the Cz electrode should be sitting directly in the middle of this distance. Then it was checked, whether the cap sits symmetrically on the participant's head. Having done the necessary adjustments, the left and right reference electrodes were connected with the sticky electrodes from before, and the chin belt was closed. Being cautious and thorough with these steps minimized the variance of channel locations among different sessions.

It mostly took some time for the temperature of the electrodes (especially the sticky reference electrodes) to match the participant's body temperature. After a short period, the signals were checked through the Unicorn Suite Hybrid Black software. Unfortunately, UHB does not support native impedance measuring, so only a signal quality estimate based on the standard deviation of the last two seconds of the signal was shown by the software. If none of the channels showed significant deviations from the rest or if there were no heavy fluctuations in the signal, it was assumed that the signal quality was good enough to proceed with the recording.

Source: https://www.unicorn-bi.com/product/unicorn-hybrid-black/
(a) Unicorn Hybrid Black EEG headset. It is a wireless system that uses Bluetooth 2.1 and consists of 8 passive dry electrodes that can be used either wet or dry.

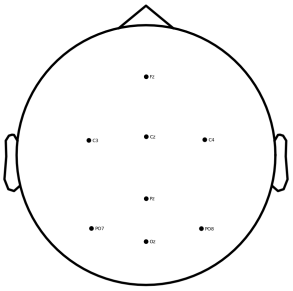

(b) Channel locations of the Unicorn Hybrid Black EEG headset. A frontal electrode (Fz) can be used for eye blink detection, whereas the electrodes over the sensorimotor cortex (C3, C4 and Cz) can be used for MI.

Figure 3.1: Unicorn Hybrid Black.

3.1.2 Eye Blink Detection

Early on in the development of the system, it was easier to test out if the eye blink detection was working as intended by looking at the real-time EEG signal of the used Fz electrode and the changing threshold for blink detection. In accordance with this realization, the experimentation of the system was adapted to accommodate testing of different feedback options. For both the single blink detection and the double blink detection systems three cases were tested: no feedback (NF), visual feedback (VF) of the signals and control feedback (CF) where the participants could control two peripherals (a vibrotactile motor and an LED) of an ESP32 circuit with their blinks.

Two healthy adult male participants (participant 1 and 2) in their early twenties attended the eye blink detection experiment. The experiment consisted of one session to test the hypothesis, whether it was possible to use the system within this only session.

3.1.2.1 ESP32

As mentioned before, one goal of this study was to research whether the developed systems could be used for home assistance applications, bearing patients with neurological disorders in mind.

For this purpose an ESP32 microcontroller was used to set up a simple circuit consisting of a vibrotactile motor and an LED. The schematic of this circuit can be seen in Figure 3.2. Then a wireless UDP (User Datagram Protocol) connection was established with the ESP32. This way, by sending either a 1 or a 0 as a byte, the Python script for the eye blink detection could wirelessly communicate with the microcontroller.

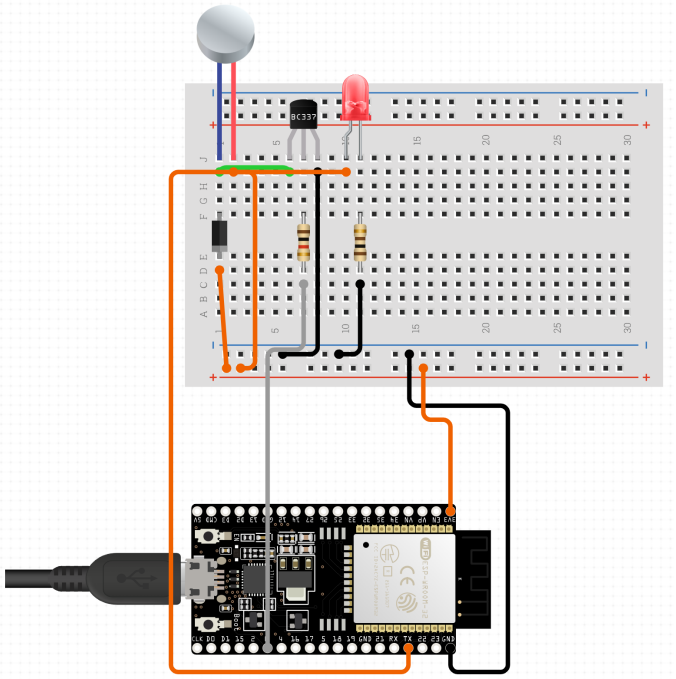

Source: https://www.circuito.io/

Figure 3.2: Circuit schematic showing the components of the ESP32 setup. The ESP32 microcontroller is connected to a vibrotactile motor and an LED. It is also connected with the eye blink detection system over a UDP connection. This allows a single blink detection to activate the vibrotactile motor and a double blink to light up the LED.

Depending on which byte was received by the ESP32, either the vibrotactile motor would vibrate or the LED would light up. This activation lasted for 0.5 s.

The purpose of this setup was that it acted as a proof of concept for an home assistance applications. For example, lighting up the LED could correspond to switching the lights on and of or turning the TV on and off. On the other hand, the vibrotactile motor could act as a bell that can be placed in the caretaker's room for the patient with neurological conditions to quickly call the caretaker. More on this can be found in chapter 6.

3.1.2.2 Single Blink Detection

As mentioned, the first part of the experiment was testing out the NF case for the single blink detection. The participants were shown two cues, either a cue to do nothing or a cue to do a single blink. These cues can be seen in Figures 3.3a and 3.3b respectively.

Before starting with the first block, the participants were asked to voluntarily blink for a few times. For each successful eye blink detection, the experimenter told the participants that they could produce a successful eye blink that could get detected by the system. This testing done for two reasons.

The first reason was to adjust the participant-specific eye blink detection threshold

parameter. The second one was to give the participants a few trial runs to get used to the system before starting with the recording. This was however limited to a maximum of five tries to reduce the effect of learning before the recording started, as the initial hypothesis was that the eye blink detection system could be effectively used without extensive training.

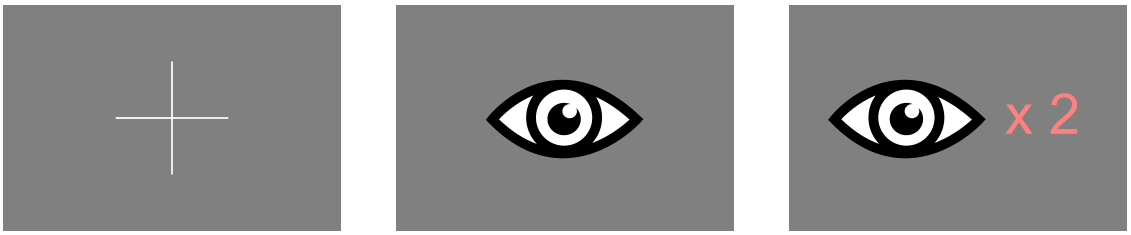

(a) Cue to do nothing. (b) Cue to do a single blink. (c) Cue to do a double blink.

Figure 3.3: Different cues shown to the participants during the eye blink recording.

After the first NF part of the experiment was over, there was a pause of 2-3 minutes for the participant to relax and get ready for the next part. This pause took place after each part during the whole experimentation so it will not be repeated for the upcoming parts.

In the second part of the experiment, the VF case was tested. Participants were shown on a second monitor the real-time signal of the Fz electrode and the moving detection threshold. They were requested once again to produce eye blinks. This way they could see for themselves how the eye blink signals looked like. They were made aware how the threshold adapted itself according to the variance of the baseline period. Then they were requested to blink exactly when a prior blink entered the baseline period. Thus they could see that the system was unresponsive during this period as the detection threshold was too high to be reached by any eye blink.

Having been introduced to how the real-time signal and the threshold interact, the participants were once again ready for the recording. Both monitors were placed directly next to each other so that the participants could keep the cues in their peripheral view while they were looking at the signal's real-time course. As there were no other distractions in the recording chamber, participants could easily focus on the signal on one monitor while keeping the cues on the other monitor in sight.

For the CF part of the single blink detection experiment, participants were first introduced to the ESP32 setup. Concretely, they were shown where the vibrotactile motor was and how it vibrated when it received a control signal. To familiarize themselves with the new setup, they were once again requested to do voluntary eye blinks for a few times. They could then see that the vibrotactile motor vibrated every time a blink was detected.

Just like for the VF, the participants were requested to keep the cues in their peripheral view while observing the motor. The circuit was placed directly in front of the monitor that showed the cues for convenience. Again, the participants could easily accomplish

the task of following the circuit's reaction and the visual cues simultaneously. The recording was started after a few trial runs.

3.1.2.3 Double Blink Detection

After the first three parts of the experiment were successfully accomplished, the double blink detection mode was activated. The participants were already familiar with the setup at this point but the double blink detection required further elaboration. As previously mentioned, if the second blink was produced directly after the first one, the amplitude of the second peak did not go as high as the first peak. This was mostly overcome by the double blink detection algorithm but participants were informed about this phenomenon. The purpose of this was to allow participants to time their second blinks better.

Since the double blink setup was not as intuitive as the single blink one, the trial run periods before each recording block were increased from five tries to eight.

After this introduction to the new setup, the three parts with different feedback options (NF, VF and CF) were repeated once again for the double blink detection. The main difference for this part of the experiment was that there was a new cue indicating that the participant should do a double blink. This cue can be seen in Figure 3.3c.

In the CF setup a single blink still made the vibrotactile motor vibrate. However, this time a double blink was used as a second control signal to light up the LED in the circuit.

Each of the six parts consisted of two blocks of 20 trials. Each cue had equal weights, meaning that for the single blink case there were 10 rest trials and 10 single blink trials. For the double blink case each of the three cues had a minimum of 6 trials, whereas two out of three cues were randomly chosen to have a seventh trial each, so that the number of trials add up to 20 again.

A trial was defined as the sum of a prestimulus period of 3 seconds, cue being shown for another 3 seconds, and a pause of 2-3 seconds. The pause duration was chosen randomly to prevent participants from anticipating a new trial. This meant that a single trial lasted about 8-9 seconds. A block was defined as a collection of trials. In this case a block consisted of 20 trials. After each block there was a small pause of 4 seconds. Taking everything into account, 40 trials were recorded for each feedback condition.

3.1.2.4 Sending Markers

Throughout the whole recording, time markers were sent from the cue and eye blink detection scripts. Every time a cue was shown on the screen, a marker with the name of the cue and the current time was written as a string value to a CSV file. The same applied for every time a blink was detected. In the case of double blink detection two different markers were sent to distinguish between a single blink detection and a double blink detection. All the scripts were run locally on a single computer.

3.1.3 Acquiring the BCI Competition IV Data Set 1

The data set used to test the feasibility of the offline analysis methods for MI was publicly available. It is provided by the Berlin BCI group [5] and can be downloaded under http://www.bbci.de/competition/iv/#dataset1.

The recording was done using BrainAmp MR plus amplifiers and an Ag/AgCl electrode cap. Recorded signals from 59 EEG positions were band-pass filtered between 0.05-200 Hz and then digitized at 1000 Hz with 16 bit accuracy. A downsampled version of the data at 100 Hz was also made available, which was used in this study.

For each participant two classes of motor imagery were selected from the three classes left hand, right hand, and foot (which foot to imagine was chosen by the participant; optionally both feet could also be imagined).

In each trial a fixation was shown for 2 s. Then visual cues (an arrow pointing either left, right or down based on the classes chosen) were superimposed on the fixation for 4 s in which the participant had to imagine moving the selected limb. After the imagery period was over, there was a 2 s pause. The data set included all the markers for the cues. For the current study only the calibration data was used both for training and testing the offline analysis methods.

3.1.4 Recording Motor Imagery Data

For recording MI data, the paradigm introduced in [6] was used. Since there are two paradigms in the mentioned study, one with and one without feedback, it should be noted that the one without feedback was adapted. From now on this paradigm will be referred to as the Graz paradigm.

As it can be seen in Figure 3.4, a trial starts with a fixation cross. After 2 s a short beep (1 kHz, 70 ms) was played indicating that a visual cue was going to show up on the screen. The cue, which was an arrow directing either to the left or to the right, was then superimposed on the fixation for 1.25 s. After the cue was shown, the participants had to imagine the corresponding hand movement for 4 s. Then there was a pause of at least 1.5 s. A value between 0 and 1 s was randomly chosen and appended to this pause period to avoid adaptation. The ending of the pause period ended the trial as well.

The only alteration done to the Graz paradigm was to match the Berlin BCI paradigm. Concretely, the minimum pause length was increased from 1.5 s to 2 s. This way both types of trials could be epoched in the same time window. It was assumed that this extra 0.5 s pause between each trial would not have any effect on the data analysis results.

Each session consisted of six blocks with 20 trials each. Each block had an equal number of class cues, meaning that in each block 10 left and 10 right hand MI trials were recorded.

In this part of the experimentation EEG data and cue markers were going to be recorded simultaneously. For this purpose the LabRecorder software was used. LabRecorder allows recording lab streaming layer (LSL) streams on the same network into a single XDF file, with time synchronization between streams. Fortunately, UHB had an LSL

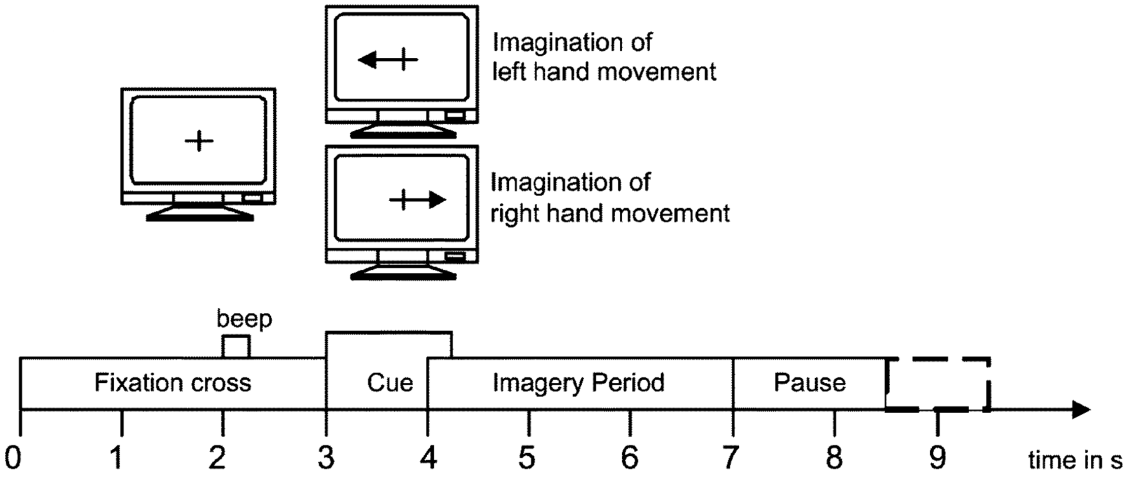

Source: Leeb et al. - Brain–Computer Communication: Motivation, Aim, and Impact of Exploring a Virtual Apartment [6].

Figure 3.4: The timing scheme of the Graz paradigm for MI recording. The steps of a full trial are illustrated. The trial starts with a fixation on the screen. Then an audible beep alerts the participant. After that a cue is shown to indicate the MI of either left or the right hand. The trial ends with a pause period.

interface. This way both the EEG data from UHB and the markers sent by the marker script could be simultaneously recorded.

The recording of EEG data from UHB could also be done through the Unicorn Suite Hybrid Black software. This way the recorded data would get saved into a CSV file. But since time synchronization of the data and marker streams was of utmost importance, LabRecorder was chosen for this task.

The EEG setup for recording MI data did not differ dramatically from the setup for the eye blink detection. The main difference was that during this experiment even more attention was paid that the participants were comfortable, as it was shown that headache and discomfort can cause a reduction in cognitive performance [39] [40]. Another rather trivial point was that the participants had to be seated in an upright position. This was shown to improve focus and the quality of the recording [41].

Prior to the recording, the participants were asked to think of two to three motions that they could imagine the easiest. They were told to try imagining doing this motion with their hands and also focusing on the sensation this motion would bring. For example, if the imagined motion was to squeeze a ball, they were asked to imagine the resistance they would feel in their hands while they were squeezing the ball.

The participants were then instructed that they should perform left hand imagery when the left cue was shown and right hand imagery when the right cue was shown. They were asked to minimize their blinks during trials and to try to blink only in the

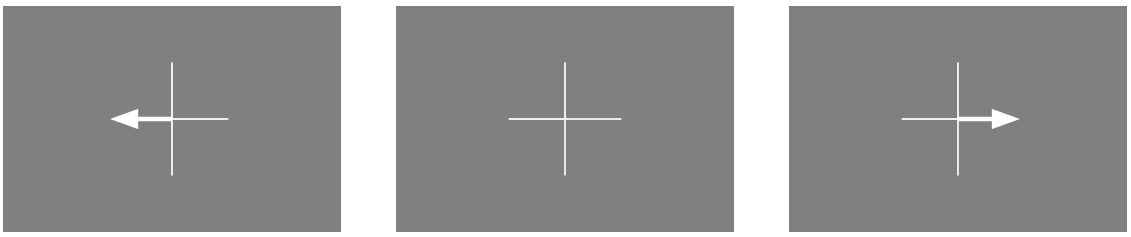

(a) Cue to perform left hand motor imagery.

(b) Fixation shown on the screen before a left or right cue. It is shown so that the participants' eye movements are minimized.

(c) Cue to perform right hand motor imagery.

Figure 3.5: Different cues shown to the participants during the motor imagery recording.

pause periods between each trial. After this initial introduction, the participants were ready for the recording.

For this part of the experiment two healthy right-handed male participants (participant 3 and 4) were recorded for four consecutive days. Each day a recording of 20 trials and 6 blocks were done for each participant, just like for the Graz paradigm. Thus, by the end of four days, there were 480 trials, 240 left hand imagery and 240 right hand imagery, for each participant.

3.2 Evaluation of the Results

The experiments were designed to make it possible to address the scientific questions posed in chapter 1. However, it was equally important to define the evaluation metrics to ensure that the experimentation results could get correctly interpreted.

3.2.1 Eye Blink Detection

The results of the eye blink detection system were evaluated based on the reaction times (RTs) and the detection accuracies. The detection accuracy metric also included the false detection rate.

RT was defined as the time difference between cue onset and blink detection. Detection accuracy was the ratio between successfully detected blinks after a cue was shown and the total number of cues. On the other hand, the false detection rate was the ratio between the number of detected blinks during rest trials or pauses and the total number of rest trials or pauses. All these metrics were evaluated separately for different feedback conditions.

The proposed metrics were suitable for answering questions 1-4 in chapter 1 because they captured the system's performance and created a common basis for comparing different feedback conditions.

Whether eye blinks could be used as control signals was addressed by combining the eye blink detections with the ESP32 and its peripherals. If the peripherals could be controlled by eye blinks, it would be assumed that detected blinks could be used as control signals for IoT devices.

3.2.2 Motor Imagery

As mentioned before, the three methods used to analyze motor imagery data were ERD/ERS, CSP, and SFBCSP.

If ERD/ERS curves similar to the ones seen in Figure 2.3a could be produced, then it would be shown that the ERD/ERS implementation worked correctly and the preprocessing of the data was helpful to highlight these features.

The expectation from CSP was that it would help classify unseen test data as either belonging to one MI class or the other. If accuracy scores of at least 10% above chance level could be acquired, then it was going to be shown that the implementation of the algorithm was working as intended. Concretely, this meant that the results would be deemed acceptable only when the accuracy scores were above 60%. If accuracy scores above 70% could be achieved, it would be concluded that good results could be obtained with CSP.

The metric SFBCSP was evaluated on was whether it would provide better accuracy scores than CSP for more than one participant. If CSP showed the desired results, SFBCSP was selected to be the next step of the pipeline to increase performance. Bearing the original study [31] in mind, a performance boost of at least 5% had to be achieved for the SFBCSP classification to be considered better than CSP. Otherwise, the high computational complexity was not considered feasible compared to normal CSP. These metrics were suitable to answer questions 6 and 7.

The evaluation metric of question 8 was whether an online system with one or two control signals using MI could be built using Unicorn Hybrid Black.

If such an MI-BCI could be built, then the answer to whether eye blinks could aid such a system would rely on adding one or two more control signals to the system using eye blinks. If only an eye blink detector could be built, this question would be addressed by discussing the possible future integration of both systems. If none of the systems could be built, the question would be left unanswered.

4 Methods and Implementation

4.1 Single Eye Blink Detection

Eye blinks appear as prominent peaks in the EEG signal. This prominence led to the idea that a simple threshold model could detect eye blinks in the signal. In other words, when the signal amplitude exceeds a certain threshold, it should be classified as an eye blink.

Early in the development, it was seen that setting the threshold too low would result in random signal fluctuations to get falsely detected as eye blinks. On the other hand, setting it too high would result in no blinks getting detected. Fixing the threshold to a suitable value before each recording seemed to have solved this issue.

However, the signal amplitude changes over time caused another issue. Sometimes after the recording started, a higher threshold was required because, for example, the electrodes could move due to too strong blinking, and thus the overall signal amplitude would increase. Alternatively, sometimes the opposite was held. After the temperature of the mastoid reference electrodes matched the person's body temperature, the noise in the signal would decrease, making the overall amplitude slightly smaller than what the threshold was initially set for.

These issues were addressed by implementing an adaptive threshold. The threshold would get updated in real-time based on the signal in a baseline window. In each iteration, the mean and the standard deviation of this baseline were calculated. A factor c was then multiplied with the standard deviation, and the result was added to the mean. This value would give the height of the current threshold.

More concretely, let T denote the threshold value, $\overline{x}_{BL}$ the mean of the baseline and σ_{BL} the standard deviation of the signal in the baseline window. Then the update rule for the threshold was defined as:

$$T = \overline{x}_{BL} + c\sigma_{BL} \tag{4.1}$$

Furthermore, let $D \in \{0, 1\}$ denote a Boolean variable specifying whether a blink was detected (1) or not (0) and x the amplitude of an arbitrary sample. Then the eye blink detection rule was defined as:

$$D = \begin{cases} 0 & x \leq T \\ 1 & x > T \end{cases} \tag{4.2}$$

Since the system worked in real-time, only the most recent samples were of interest when looking for an eye blink. Concretely, this meant that it was enough to apply

equation 4.2 to a small window at the very end of the signal buffer, called the activity window. Lastly, since the goal was to detect single eye blinks and such eye blinks appeared as singular peaks, the maximum value in the activity window was enough to use as the sample amplitude x in equation 4.2.

These steps were done after band-pass filtering the signal between 1-30 Hz and applying a moving average filter to smoothen the signal. For band-pass filtering, a one-pass, zero-phase, non-causal filter was used. As the filtering was done on data buffers, using a non-causal filter was possible. Following the recommendations from [42] and [43], the filter parameters can be reported as:

- Hamming window with 0.0194 passband ripple and 53 dB stopband attenuation
- Lower transition bandwidth: 1.00 Hz (-6 dB cutoff frequency: 0.50 Hz)
- Upper transition bandwidth: 7.50 Hz (-6 dB cutoff frequency: 33.75 Hz)
- Filter length: 825 samples (3.300 sec)

As moving average filters act as low-pass filters, it was rather an optional step to apply it for better visualization. It has to be noted that other smoothing filters, e.g., Gaussian filter, could be used for this purpose as well, but they were not tested out in this study.

Although it was shown that high-pass filters above 0.1 Hz deteriorate the waveform of EEG signals [44] [43], as mentioned, 1 Hz was selected for this implementation. There were three main reasons for this decision.

The first reason was that eye blink signals are muscle artifacts and not brain signals. This made it irrelevant whether the filtering distorted the waveform, as long as the filtered signal was used only for eye blink detection. While the system was running, raw EEG data could still be accessed. This meant that the signal could be filtered again with a different cutoff frequency for another application, e.g., for MI.

Second, it was intended that the system only detected intense, voluntary eye blinks and not the spontaneous ones that the user cannot prevent. This phenomenon can be seen in Figure 4.1. The small peaks around the samples 800, 2100, 2900, 4100, and 4800 were spontaneous eye blinks. They did not get detected because they were sub-threshold peaks. On the other hand, the peaks around 1100, 1800, and 3300 were voluntary single blinks with large amplitudes exceeding the detection threshold, thus getting detected as eye blinks. A 1 Hz high-pass filter was suitable for this task, as it "squished" these small amplitude peaks and kept only the voluntary peaks intact.

Lastly, a high-pass filter with a lower cutoff rate requires a longer filter, i.e. more samples to operate on [45]. Concretely, a 0.1-30 Hz band-pass filter would have the length of 8251 samples, which was larger than the buffer size of 5000 samples. The buffer size might have been increased to use this filter but this would result in an overall slower system. This was because the filtering would require more computing power and also there would be more samples to filter. Since this was an online system that operated with signal buffers in quasi real-time, keeping the system as light as possible was desirable.

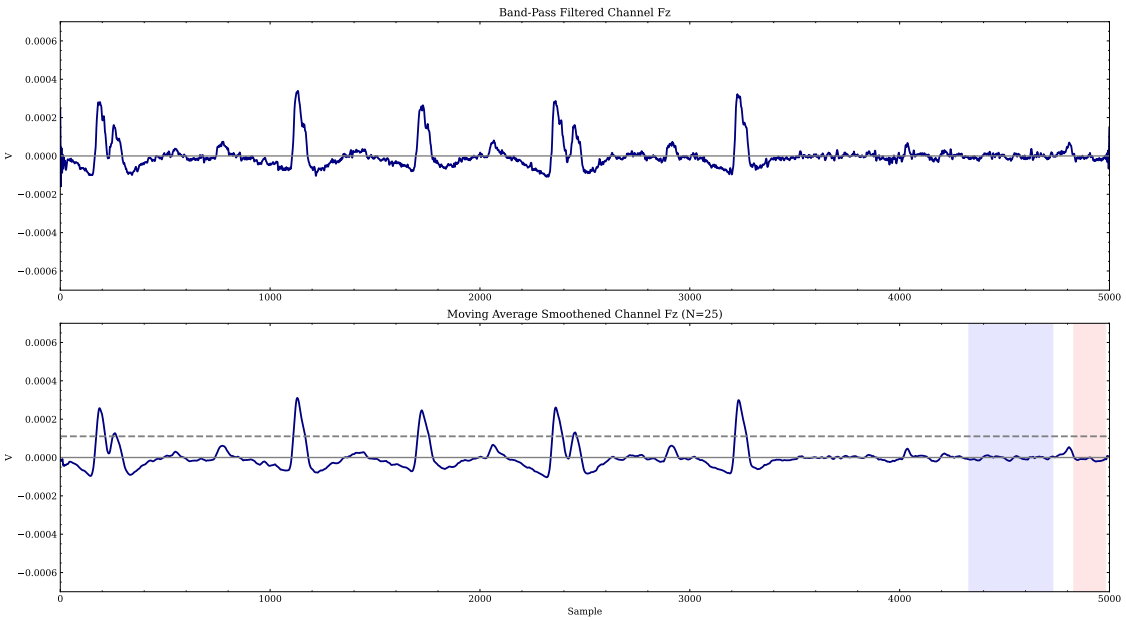

Figure 4.1: Different types of eye blinks seen in the frontal channel. New samples arrive in the buffer from the right. The blue window corresponds to the baseline and the red to the activity window. Small peaks around samples 800, 2100, 2900, 4100, and 4800 are sub-threshold spontaneous blinks, i.e., they do not get detected as eye blinks. Peaks around the samples 1100, 1800, and 3300 are voluntary single blinks with large amplitudes exceeding the detection threshold, thus getting detected as eye blinks. The peaks around the samples 200 and 2400 are double blinks. It can be seen that the second blink has slightly less amplitude than the first.

One of the biggest disadvantages of using a buffer was the existence of edge artifacts due to filtering [42]. They can be seen at the start and end of recordings. These artifacts occur because filters try to access samples that are not available. To solve this issue it is recommended that recordings should start earlier and end later than planned, so that only these empty periods get affected by edge artifacts and can later get cropped out [43]. But this cannot be done in an online setting where only fixed signal buffers are available.

These artifacts could be ignored but unfortunately the random fluctuations that they cause would sometimes result in a false blink detection. Therefore, a small delay of 20 samples (0.08 s for 250 Hz sampling rate) was introduced to the activity window. This delay was short enough that the users would not even recognize it but sufficient to solve the problem of edge artifacts.

The introduced delay can be seen in Figure 4.2. This figure shows the zoomed in end of the signal. As it can be seen, filtering caused an edge artifact which persisted even after smoothing the function. The short delay accounted for this small residual. Due to this delay, the most recent samples reached the red activity window, starting around

sample 4850, only after 0.08 s.

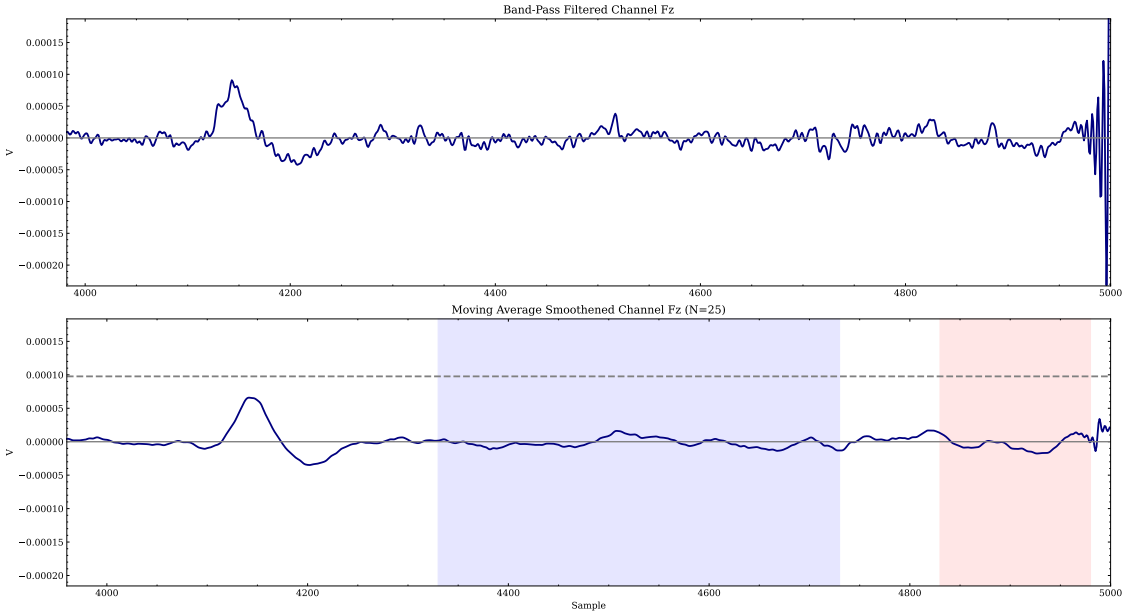

Figure 4.2: Edge artifacts due to filtering. At the edge of the buffer, filtering artifacts can be seen due to the filters trying to reach for samples that are not yet available. A short delay was introduced to the system to overcome the issue of false blink detections due to such artifacts. This delay causes the activity window to be shifted slightly to the left.

The last part of this detection algorithm was the implementation of a "refractory period" for blink detection. Without this period, a blink that the system detected would keep on getting detected as a new blink until it exited the activity window. This was because the threshold would not yet get updated until the detected peak entered the baseline period and increased the standard deviation of the baseline signal. By making the system go into a refractory period until the peak exited the activity window, this issue could get resolved.

Concretely, the program would run a predefined number of iterations doing nothing and waiting for the refractory period to be over. This part was crucial for later, when the system would send control outputs to the ESP32 microcontroller to activate a vibrotactile motor. Without the refractory period, the motor would vibrate not only once, but as many times as the blink would get detected until it exited the activity window.

4.2 Double Eye Blink Detection

The double blink detection system acted in similar terms to the single blink detection system. The detection of a blink using a threshold value was exactly the same as before. But this time detecting one blink would not directly cause a single blink detection to be triggered. If this was the case, there would be no time to detect a secondary blink.

Therefore, a waiting period was implemented where the program would wait for a second blink to occur. If a second blink was not detected in a predefined amount of iterations, a single blink detection signal would get triggered. Otherwise, a double blink would get detected and the corresponding control signal would get triggered. But the detection of a second blink needed some special care.

As it can be seen in Figure 4.1, blinks after the first blink had smaller amplitudes. This meant that the threshold for the first blink detection would most probably be too high for consecutive blinks. Thus, after the first blink got detected the threshold value was halved. Then an automatic peak finding algorithm provided by the SciPy Python library [46] was run. If two peaks were counted in the activity window during the waiting period a double blink detection signal was triggered.

The question may arise whether it would be feasible to exclusively use this algorithm for peak detection. But it was observed that this was computationally more expensive than using a simple threshold value for single blink detection, especially when done in real-time in each iteration. This sometimes caused the peaks to exit the activity window, before they could even get detected, i.e. missed blink detections. Therefore, this peak finding algorithm was only used for finding multiple blinks after a first one was detected.

Another thing to adapt was the activity window. In the single blink detection, the activity window was chosen to be as short as possible so that the baseline window was not too far away from the most recent signals and the system would depend on its recent past. But this resulted in some some double blinks getting unnoticed because the first blink would exit the activity window before a consecutive one could enter it. So the activity window was made wider to allow multiple blinks to fit in.

4.3 Processing of EEG Data for MI

The second part of this study consisted of the investigation of MI signals. For this purpose first the publicly available BCI Competition IV-1 data set and then the recorded data set was analyzed. For the EEG data analysis the MNE Python library [47] was used.

4.3.1 BCI Competition IV-1 Data Set

The analysis of the BCI Competition IV-1 data set consisted of three parts: ERD/ERS analysis, CSP and SFBCSP. For the ordering of the processing steps mostly the recommendations from [43] were followed.

As discussed before, the first step of ERD calculation was to band-pass the signal in the frequency band of interest. Since the focus was on the mu-band, continuous EEG data was band-pass filtered in the 8-12 Hz band. For this purpose a one-pass, zero-phase, non-causal FIR filter was used with the following parameters:

- Hamming window with 0.0194 passband ripple and 53 dB stopband attenuation

- Lower transition bandwidth: 2.00 Hz (-6 dB cutoff frequency: 7.00 Hz)
- Upper transition bandwidth: 3.00 Hz (-6 dB cutoff frequency: 13.50 Hz)
- Filter length: 165 samples (1.650 sec)

Then the continuous data was epoched between 2 s before the cue onset and 6 s afterwards.

Assuming that the Unicorn Hybrid Black recordings would be noisy and require either interpolating bad channels or rejecting trials, an automatic way of doing these operations had to be tested to make sure that they worked as intended. For bad channel interpolation, RANSAC (random sample consensus) [48] from the PREP pipeline [49] as re-implemented in the autoreject Python library [50] was used. For automatic rejection of trials autoreject library itself was used.

The aim of automating the whole pipeline as much as possible was to be able to transfer the methods used on the "ideal" data set to the data set recorded with the Unicorn Hybrid Black.

Lastly, for the broad-band CSP, raw continuous EEG data was band-pass filtered between 4-40 Hz with again a one-pass, zero-phase, non-causal FIR filter was used with the following parameters:

- Hamming window with 0.0194 passband ripple and 53 dB stopband attenuation
- Lower transition bandwidth: 2.00 Hz (-6 dB cutoff frequency: 3.00 Hz)
- Upper transition bandwidth: 10.00 Hz (-6 dB cutoff frequency: 45.00 Hz)
- Filter length: 165 samples (1.650 sec)

4.3.2 Recorded Data Set

The methods used to analyze the data set recorded with the Unicorn Hybrid Black were nearly identical to the ones to analyze the BCI Competition IV-1 data set. Also the band-pass filters used were kept the same. There were only three differences between these pipelines.

First difference was that a notch filter had to be applied to the data. Unicorn Hybrid Black was very susceptible to the 50 Hz line noise and its harmonics. Band-pass filtering the signal was not enough to get rid of this interference. That is why an additional notch filter was applied to the frequencies 50 and 100 Hz. The power spectral density plots before and after filtering can be seen in Figure 4.3. Only band-pass filtering did not remove the line noise at 50 Hz. Also there was some residual interference around 100 Hz. An additional notch filtering cleared most of this noise.

The second difference was that the signal had to be cropped after filtering. This was because there were extensive periods of data at the start and end of each recording. Again, this was intentionally done to minimize edge artifacts.

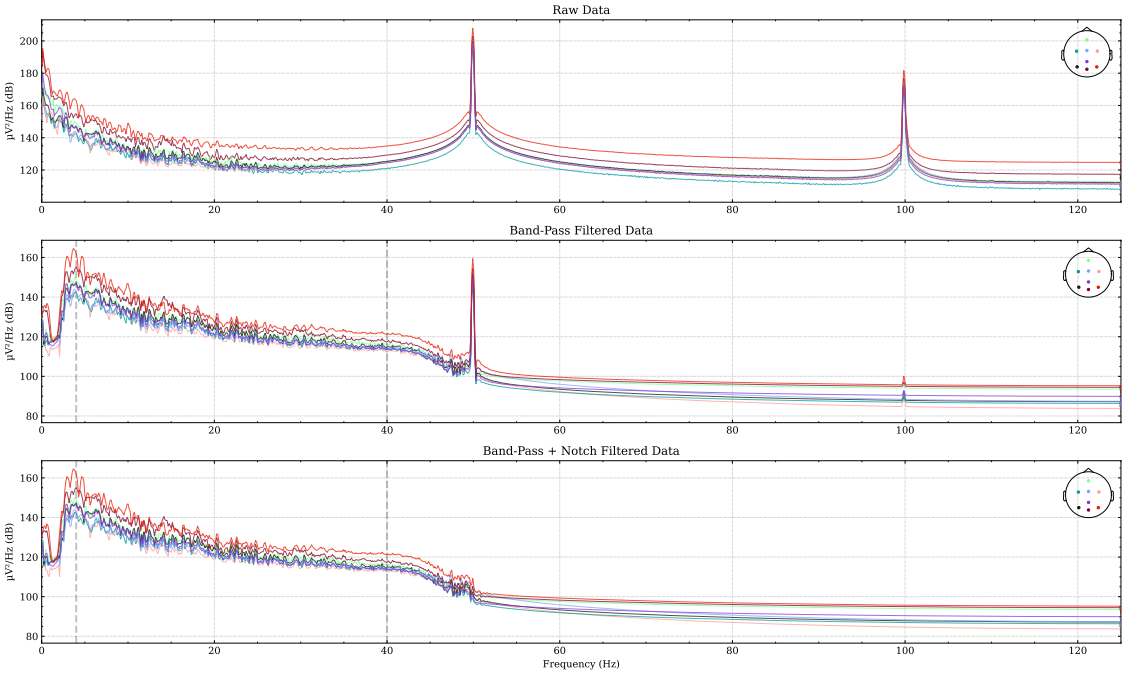

Figure 4.3: Filtering effects on the PSD plots. Unfiltered (raw) data is contaminated by line noise at 50 Hz and its harmonics at 100 Hz. 4-40 Hz band-pass filtering the signal reduces the 100 Hz interference, but the 50 Hz noise remains intact. A combination of the notch and band-pass filtering eliminates most of the noise.

And lastly, of course the timing of the paradigm was slightly different. Here there were two main differences. First, the prestimulus period was 3 s long with an audible beep to alert the participant instead of 2 s without any audible beep. Second, the visual cue would not remain on the screen for the whole imagery period but would rather disappear after 1.25 s.

These were very negligible changes and there was no loss of information due to different timings since the epoched window of -3 to 6 s for the recorded data set contained the -2 to 6 s window of the Berlin BCI data set (-3 and -2 s refer to seconds before the cue onset). This means that fundamentally the paradigms were doing the same thing and consisted of the same periods with only 1 s extra prestimulus data for each epoch for the recorded data set. But this extra second could be discarded from epoching, making both epochs the same length. This meant that the results applied to one data set should be transferable to the other and that results from both data sets could be compared on a common basis.

5 Results

5.1 Single Blink Detection

As mentioned in chapter 3, the blink detection system's performance was evaluated based on reaction time (RT) and detection accuracy.

For the single blink detection case, RT results from both participants are shown in Table 5.1 and visualized in Figure 5.3. Participant 1 could achieve an average RT of 1.07 s across different feedback conditions, whereas it was 0.9 s for participant 2. Thus the RT of single blink detection was approximately 1 s.

Table 5.1: Single Blink Detection Reaction Times
(Best are marked in bold).

	Participant 1	Participant 2
No Feedback	**1.02 s ± 0.30 s**	**0.87 s ± 0.08 s**
Visual Feedback	1.06 s ± 0.27 s	0.91 s ± 0.14 s
Control Feedback	1.13 s ± 0.22 s	0.92 s ± 0.11 s

The best RTs were achieved for the case with no feedback (NF). But since the mean differences between different conditions were rather very small (max. 110 ms), it can be concluded that the feedback had virtually no effect on the RT of the system.

As a further metric, detection accuracies are shown in Figure 5.1. For each participant-condition pair different periods of the recording are shown on the x-axis and the detection accuracies on the y-axis. As a reminder, the participants were instructed to voluntarily blink every time a blink cue was shown and not to do so after rest cues. What the participants were unaware of during the recording was that the pauses between trials would also be taken into account when computing the results.

Considering that there are 20 trials per cue, a minimum detection accuracy of 75% was acquired. The lowest detection accuracy was detected for the visual feedback (VF) condition of participant 1. But this low accuracy was mostly due to this recording being very noisy. Between NF and VF, this participant took off his blazer, moving the reference electrodes on the mastoids as a result. This resulted in five blinks getting unrecognized. Only after the VF period was over, the problem was identified and the mastoid reference electrodes were re-applied. This had a direct impact on the results from the control feedback (CF) case, which showed the best detection accuracy for participant 1. In short, the low accuracy of VF for participant 1 was due to bad referencing but was then fixed for CF.

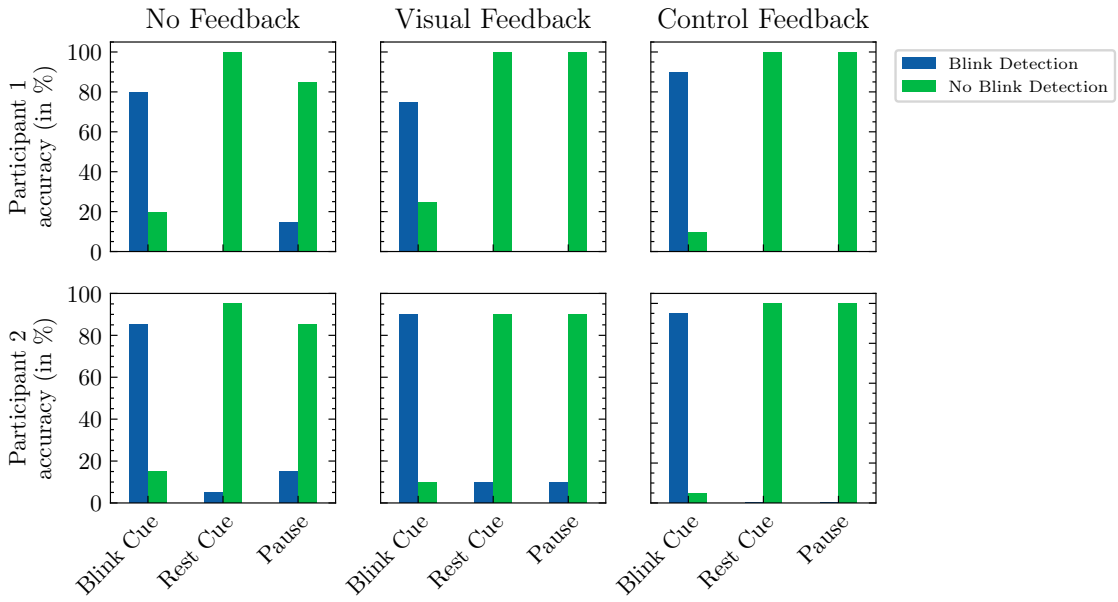

Figure 5.1: Detection accuracies of the single blink detector for different feedback conditions. It can be seen that both participants could reliably produce voluntary eye blinks after a cue was shown to do so. Furthermore the false detection rates (falsely detecting a blink) very low across all conditions.

Shifting the focus to rest cues shows that the maximum false detection rate was 10%. This rate increases to 15% when also the pauses were taken into account. Pause periods gave a very good estimate of the false classification rate for real-life scenarios. This was because the participants were not paying the same attention not to produce voluntary blinks as in rest periods. This is similar to users "forgetting" that the system is on in a real-life theoretical scenario. That is why pause periods could be seen as worst-case scenarios and that the false detection rate of the system in these periods was a precious result.

Although the RTs were the highest for CF with circa 100 ms delay compared to peak RTs, the accuracies told a different story. For both participants, both the highest detection accuracies and the lowest false detection rates were achieved in this condition. Concretely, the false detection rates were 0% for both participants and missed detection rates were 10% for participant 1 and 5% for participant 2.

Summarized, the results showed that for both participants the accuracies and RTs were rather uniformly distributed with low false detection and high detection rates.

5.2 Double Blink Detection

Analogously, the RT results for the double blink detection can be seen in Table 5.2 and again these results are plotted in Figure 5.3.

Table 5.2: Double Blink Detection Reaction Times
(Best are marked in bold).

		Participant 1	Participant 2
Single Blink	No Feedback	1.81 s ± 0.24 s	1.78 s ± 0.29 s
	Visual Feedback	1.75 s ± 0.15 s	**1.60 s ± 0.18 s**
	Control Feedback	**1.68 s ± 0.13 s**	1.84 s ± 0.15 s
Double Blink	No Feedback	1.46 s ± 0.11 s	**1.26 s ± 0.23 s**
	Visual Feedback	1.41 s ± 0.09 s	1.37 s ± 0.18 s
	Control Feedback	**1.28 s ± 0.09 s**	1.38 s ± 0.25 s

The results show that the RTs for double blinks were better than single blinks. The reason for that was the implementation of the double blink detection algorithm. As explained in chapter 4, in the double blink detection case, there was a short waiting period after the first blink was detected for the second blink to arrive. In the implementation of the algorithm, this period was defined as 10 while loop iterations which corresponded to 0.5-0.7 s depending on the system load. It was thus reflected in the increased RTs for the single blink detection.

This time there was no clear cut which feedback condition gave the best RT among participants. It can be observed that participant 1 had the fastest RT for CF. At first sight, it seemed like there was no consensus to which feedback condition provided the best RT for participant 2. But this required further attention.

As it can be seen in Figure 5.2, nearly half of single blinks were detected as double blinks. This was due to a poor setting of a participant-specific parameter. As discussed before in chapter 4, the detection threshold for second blinks had to be decreased due to the second peak being lower than the first. This parameter was first adjusted for the noisy signal of participant 1 but not re-adjusted for participant 2 in the beginning of the experiment. Since the recording of participant 2 was very clean, the threshold was decreased way too much after each blink detection. This caused even the slightest increase in the signal to be detected as a second blink. And for most of the trials, this increase came directly after the first blink. Thus there were a lot of false double blink detections which accounted for the low RTs. Thus it became evident that NF having the fastest RT for participant 2 was just due to poor parameter selection.

Of course, the mentioned parameter was corrected after the NF session which increased the detection accuracy performances again. Unfortunately NF could not be re-recorded, both because of time constraints and to minimize the inter-session learning effect.

It could be observed that for the double blink detection case false detection rates during rest periods and pauses were virtually 0%. It can also be seen that an intended double blink was detected as a single blink more than the opposite case. This is not the case only for NF condition of participant 2 but it was explained that this was rather

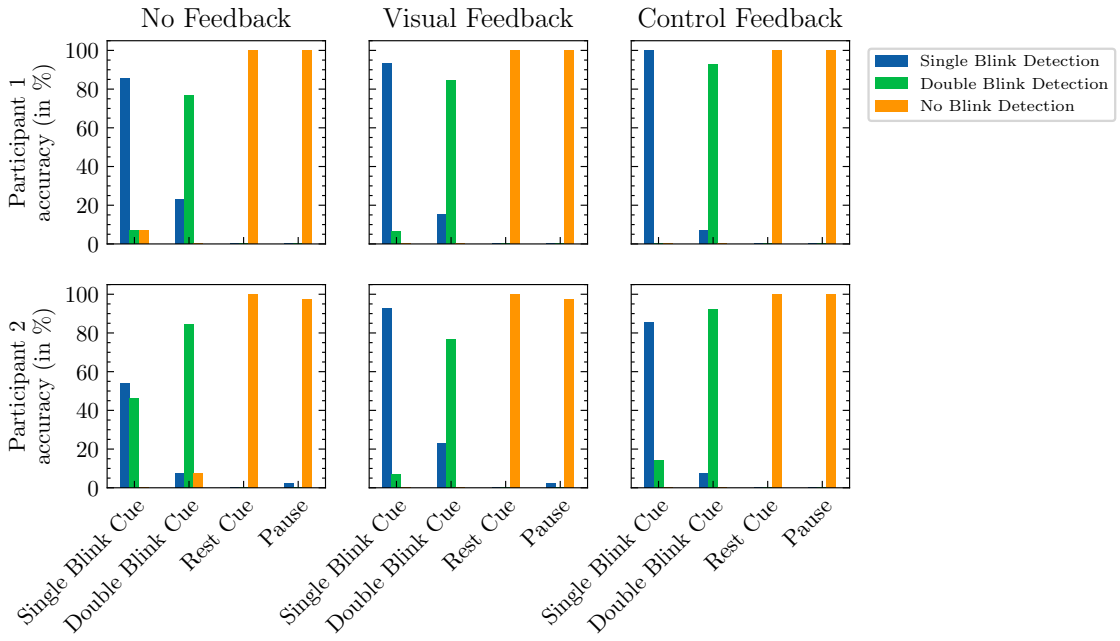

Figure 5.2: Detection accuracies of the double blink detector for different feedback conditions. It can be seen that both participants could reliably produce the correct voluntary eye blinks after the corresponding cue was shown. Furthermore the false detection rates (falsely detecting a blink) were very low across all conditions (virtually zero). The band performance of single blink cues in the NF condition of participant 2 was due to poor selection of participant-specific parameters for the setup.

due to false parameter settings. Again, the CF seemed to show the best results when it came to detection accuracy, both in terms of correct intended motion recognition and low false recognition rates.

Finally, looking at Figure 5.3 shows again that for both participants the best RTs were achieved with a single blink detection system. The slowest RTs were seen for the single blink detections in the double blink detection system due to the waiting period discussed earlier.

5.3 Offline Analysis of the BCI Competition IV-1 Data Set

The BCI Competition IV-1 data set was analyzed as a test case to see how the methods proposed in previous studies performed and whether it was feasible to use them on the data set recorded with the Unicorn Hybrid Black. The results show the ERD/ERS curves for different participants and the accuracy scores for both CSP and SFBCSP.

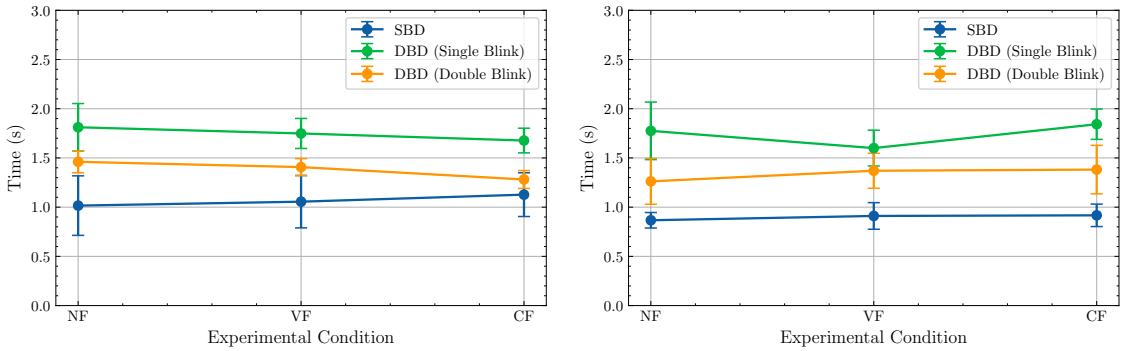

(a) Reaction times of participant 1 for different feedback conditions.

(b) Reaction times of participant 2 for different feedback conditions.

Figure 5.3: Reaction times of both participants for different conditions. SBD: single blink detector, DBD, double blink detector. The results show that the single blink detector had the best RT because the system would register a detected blink as soon as the blink was detected. This was not the case for the single blink detection of DBD because here the system was waiting for a second blink to occur before registering a single blink. Consequently, the single blink detection of DBD had the worst RT. However, for both participants the mean RTs were lower than 2 s across all feedback conditions.

5.3.1 ERD/ERS Curves

ERD/ERS curves of different participants' left and right hand MI signals were plotted for three electrodes on the sensorimotor cortex (C3, Cz and C4) before and after spatial filtering. For each plot x-axis shows the time in seconds. 0 corresponds to the time when the visual cue was shown to the participants. On the y-axis is the relative power in percentage.

Figure 5.4a shows that there was no clear distinction between left and right MI. The prominent peak at around 5.5 s was most probably an eye blink. It is highly possible that the participant blinked approximately around the same time at the end of every trial and the averaged epochs retained these peaks.

After applying spatial filtering the results look very different. Figure 5.4b shows the ERD/ERS curves after CAR. As it can be seen, the classes could be easily separated from each other.

As expected, C3 showed an ERD of right hand MI starting after about 0.5 seconds after the cue onset and remained for about 3 seconds. Analogously C4 showed a symmetric ERD for the left hand MI. Even after spatial filtering there was nearly no difference between the two classes for the Cz electrode. Bearing the cortical homunculus in mind, it was expected that there was no ERD observed in Cz, as it is far away from areas related to the hands. As it will be introduced below, participant E unsurprisingly had the highest accuracy score on all tested methods.

However these ideal looking ERD/ERS curves could only be seen for participant E.

As a contrast, the ERD/ERS curves of a worse performing participant B can be seen in Figures 5.5a and 5.5b. The clear-cut distinction between different classes seems to have disappeared. There is also a distinctive peak in 3-4 s period which got pressed down due to the smoothing of the ERD/ERS curves. Most probably, this peak was also generated by overlapping eye blinks across epochs. Comparing both figures, it can be seen that CAR worked as intended because it clearly discarded this artifact and highlighted the distinction between different classes (even though this was a faint distinction).

Although these curves did not look as clean as for participant E, as mentioned, a distinction between classes can still be made. Looking carefully, it could be seen that the time period between 2-4.5 s still behaved as expected: C3 showed a stronger ERD for right hand MI and C4 showed a stronger ERD for left hand MI. This observation came in handy during CSP computation.

These examples clearly demonstrated that each participant behaved differently. Although a very good result could sometimes be seen for one participant, supporting the homunculus for example, the same result could be very faint or might have not appeared at all for others. When it comes to BCIs an all-in-one solution is very difficult to come by.

5.3.2 CSP

CSP was applied to the data to classify between different classes of MI. Table 5.3 shows the test set accuracies of different classifiers for different participants. These results were obtained by band-pass filtering raw EEG data between 4-40 Hz and epoching the filtered data in the window of 0.5-2.5 s. The parameter m in equation 2.15 was chosen to be 2. The features were used to train three different classifiers: support vector machine (SVM), linear discriminant analysis (LDA) and logistic regression.

Table 5.3: Broad-band CSP accuracies for the BCI Competition IV-1 data set for 0.5-2.5 s epoching (Best are in bold).

	Subject A	Subject B	Subject C	Subject D	Subject E	Subject F	Subject G
SVM	0.77	**0.55**	0.6	**0.83**	**0.97**	**0.8**	**0.92**
LDA	**0.87**	0.53	**0.63**	**0.83**	**0.97**	0.77	0.9
Logistic Regression	0.85	0.53	0.57	0.82	0.93	0.78	**0.92**

It can be seen that all participants performed above chance level (50%) and except for participant B, who had a peak accuracy of 57%, all the participants passed the predefined evaluation metric of at least 60% accuracy. Five participants even performed above 70% which was another predefined evaluation metric for how well the method performed. It is remarkable that participant E achieved a peak accuracy score of 97%.

The bad performance of participant B was in line with previous ERD/ERS findings. Figure 5.5b shows that there was no discriminative power in the 0.5-2.5 s window. Thus

it was of interest whether extending the current window with the aforementioned 2-4.5 s window would boost the performance of participant B.

Table 5.4 shows that this was indeed the case. Extending the epoching window to cover the window with the most discriminative power increased the peak accuracy by 18% for participant B. Actually, participants C, D, E and F have also benefited from this change. Participant E even achieved a 100% test set accuracy. Of course, this should not be mistaken for an all encompassing classifier for this participant. Proving this point, the mean score for a 20-fold cross-validation of this classifier was actually 98.57%.

Table 5.4: Broad-band CSP accuracies for the BCI Competition IV-1 data set for 0.5-4.5 s epoching (Best are in bold).

	Subject A	Subject B	Subject C	Subject D	Subject E	Subject F	Subject G
SVM	**0.85**	0.65	0.67	0.9	**1.0**	**0.87**	**0.48**
LDA	**0.85**	0.65	**0.7**	**0.92**	**1.0**	0.83	0.42
Logistic Regression	0.83	**0.72**	**0.7**	**0.92**	**1.0**	0.85	0.4

Another interesting phenomenon was the decrease of accuracies for participant G. This shows that more data is not always better. The general conclusion is that each participant's neurophysiological data looked different and they should be handled individually.

Looking at Tables 5.3 and 5.4, LDA and SVM seemed to have worked very well for the first case, whereas logistic regression performed generally better in the case with a wider epoching window. However, in both cases peak performances for each participant were achieved with different classifiers. This meant that choosing participant-classifier pairs carefully could account for some performance boost. Taking into account that all three classifiers were linear classifiers, it was remarkable that high-dimensional and complex EEG data could be linearly separable after proper preprocessing.

5.3.3 SFBCSP

In the next step, results computed from CSP were compared with the ones from SFBCSP. For this purpose the original epoch of 0.5-2.5 s was used. As SVM had the best overall results in Table 5.4, it was adapted for SFBCSP as well. The comparison of CSP and SFBCSP scores can be seen in Table 5.5.

The results show that the implemented SFBCSP could achieve better results for most participants. Bearing the predefined evaluation metric of at least 5% accuracy boost in mind, it can be said that SFBCSP passed this test for four out of seven participants.

Participant E was a special case where the performance was already very high and could not allow a 5% increase. This case was not considered in the evaluation. However, seeing that the high performance of participant E was retained by the SFBCSP, it can be assumed that it passed the test for participant E as well.

Table 5.5: Comparison of SFBCSP and CSP accuracies for the BCI Competition IV-1 data set for 0.5-2.5 s epoching
(Best are in bold).

	Subject A	Subject B	Subject C	Subject D	Subject E	Subject F	Subject G
CSP	0.77	0.55	0.6	0.83	**0.97**	**0.8**	0.92
SFBCSP	**0.92**	**0.7**	**0.72**	**0.9**	**0.97**	0.5	**0.93**

The most significant increase in accuracy came from participants A and B with 15%. However, there was a considerable decrease in the performance of participant F. Comparing the Lasso coefficients for different participants shed some light on this difference.

As it can be seen in Figure 5.6, the current implementation of SFBCSP was not particularly sparse. For example, for participant B nearly all the features were used by the classifier. This contrast between results from the current study and the results from the original study became even more obvious when Figure 5.6 was compared with 2.5.

Focusing on the current study again, the plot for participant A in Figure 5.6 showed that there was some sparsity but not as much as for participant F. Most probably, this significant sparsity of the feature vector for participant F caused the decrease in the classifier performance. This was unintuitive, as SFBCSP was designed to have sparse feature vectors. However Table 5.5 shows, for example, the promising results obtained by non-sparse feature vectors for participant B. These results suggested that choosing the sparsity parameter λ manually may be beneficial. But this was not investigated in this study to keep the whole pipeline as automatic as possible. It was assumed that this way it would be easier to transfer the results from the BCI competition data set to the recorded data set.

5.4 Offline Analysis of the Recorded Data Set

The methods tested on the BCI Competition IV-1 data set were then applied to the data set acquired with the Unicorn Hybrid Black.

5.4.1 ERD/ERS Curves

Figures 5.7 and 5.8 show the ERD/ERS curves of two different recording sessions. The plots show that the data was very noisy even though heavy smoothing was applied. It can also be seen that the relative power of the curves was not in the same range with the ideal curves in Figure 5.4. The curves from the BCI competition IV-1 data set would decrease down until -25% to -50% but the lowest ERD for the recorded data set could be seen in 5.7b with only a -20%.

Furthermore, there was hardly any period of time where the classes could be discriminated from each other. Even after spatial filtering, all the the relative powers of each

channel followed nearly the same course. C4 from Figure 5.7b showed that there was a slightly larger ERD for left hand MI than right hand MI, which was in line with the expectation from the homunculus. Also Figure 5.8b showed that either C3-Cz or C4-Cz might be a good basis for discrimination. But these observations were not helpful when it came to the actual classification of the signals.

The most curious part was that the pre-stimulus period showed some activity in the -2 to 0 s range. For both recordings the relative band power started decreasing at around -1 s (C3 and C4 in Figure 5.7b, C4 in Figure 5.8b) However, neither baseline correction nor detrending helped with the issue. This led to the question whether there could be an asynchrony in the cue markers. A possible reason for this phenomenon could, for example, be that the markers were sent 1 second too late. Considering this possibility, the ERD/ERS curves were plotted again. However, the results looked nearly the same and for the sake of conciseness these plots were not included.

5.4.2 CSP

Bearing in mind that there seemed to be little valuable information in the ERD/ERS curves, CSP was applied to the data set to see if it would produce any better results. The resulting accuracy scores can be seen in Table 5.6.

Table 5.6: Broad-band CSP accuracies for the recorded data set (Best in bold).

		Session 1	Session 2	Session 3	Session 4
Participant 3	LDA	**0.54**	**0.41**	0.43	**0.48**
	SVM	0.51	**0.41**	**0.53**	**0.48**
	Logistic Regression	0.49	**0.41**	0.40	0.46
Participant 4	LDA	0.43	0.47	0.38	0.50
	SVM	0.46	**0.53**	**0.54**	**0.52**
	Logistic Regression	**0.54**	**0.53**	0.50	0.49

The results show accuracy scores around the chance level. Since it was previously defined that an acceptable result would have at least 60% accuracy, none of the results can be deemed acceptable. The pipeline was tested with different parameters for epoching, baseline correction and classifiers. However, the results did not significantly deviate from chance level. So, they were not included in this study for the sake of conciseness.

5.4.3 SFBCSP

As a last step, SFBCSP was applied to observe if it produced any better results. Table 5.7 shows these results.

It can be seen that SFBCSP was not useful in this case. There was a 5% increase in accuracy for only one session-participant pair. If the classifiers would not perform

Table 5.7: Comparison of SFBCSP and CSP accuracies for the recorded data set (Best are in bold).

		Session 1	Session 2	Session 3	Session 4
Participant 3	CSP	**0.51**	0.41	**0.53**	0.48
	SFBCSP	0.40	**0.52**	0.41	**0.53**
Participant 4	CSP	0.46	**0.53**	**0.54**	**0.52**
	SFBCSP	**0.48**	0.40	0.42	0.45

around chance level, this would be counted as a successful SFBCSP accuracy boost. However this would not be a good conclusion in this case, as the increase might as well have happened due to random effects and not due to proper functioning of the algortihm.

As expected, these results showed that SFBCSP cannot boost CSP performance for the recordings done with the Unicorn Hybrid Black. This is not surprising as CSP was not producing good results to start with.

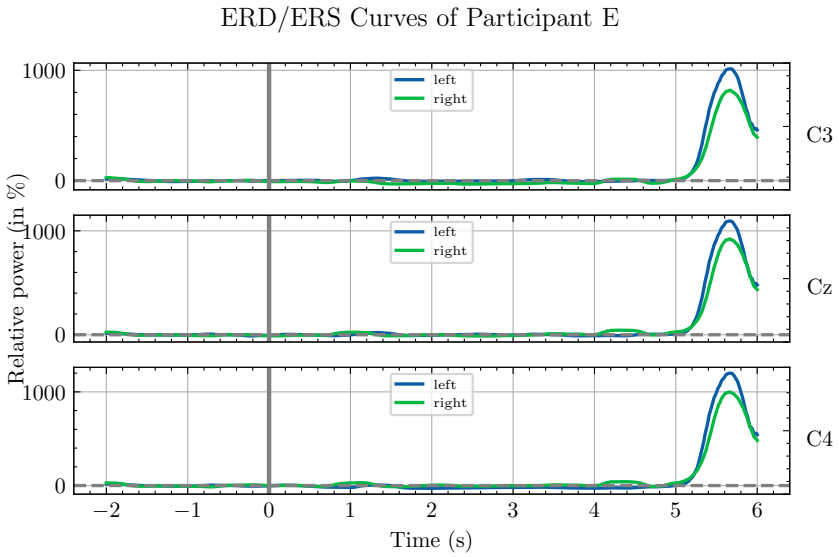

(a)

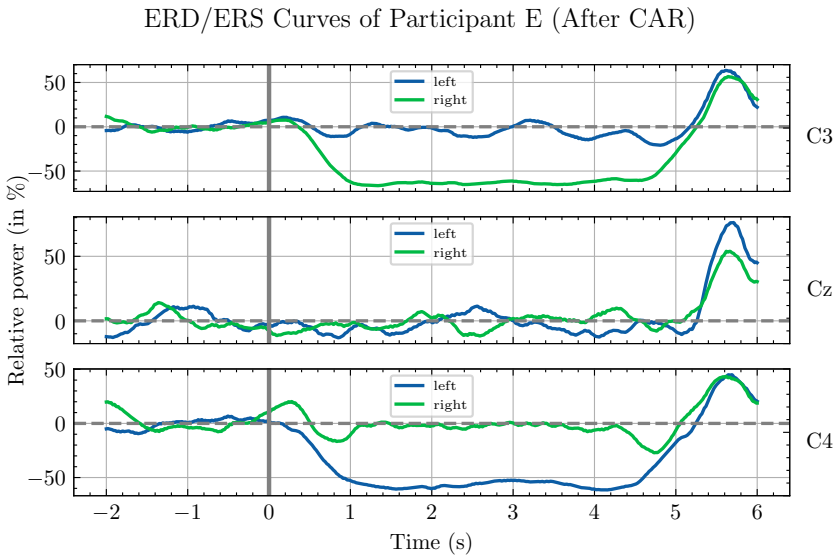

(b)

Figure 5.4: ERD/ERS curves of participant E for different motor imagery tasks. Each subplot shows a different channel on the sensorimotor cortex. (b) shows that spatial filtering made it possible to separate different classes from each other. After CAR, ERDs that lasted for ca. 3 s could be observed in channels C3 and C4, in line with the expectations from the homunculus.

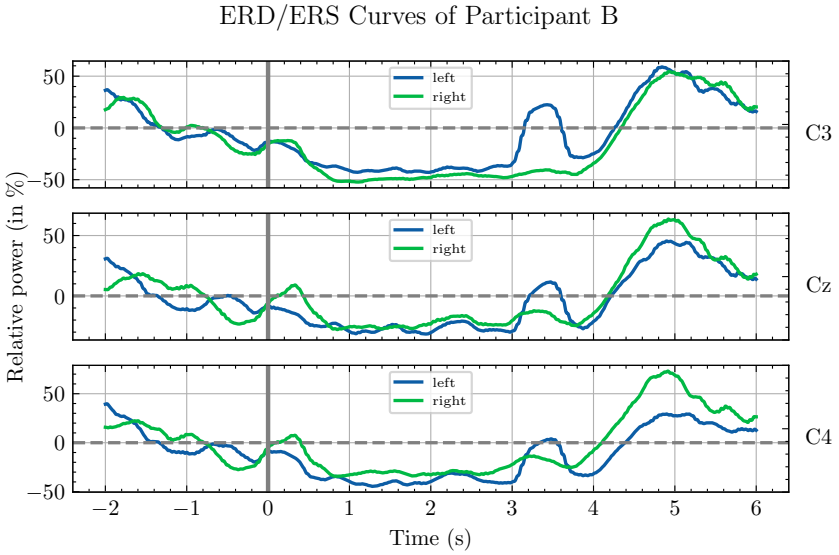

(a)

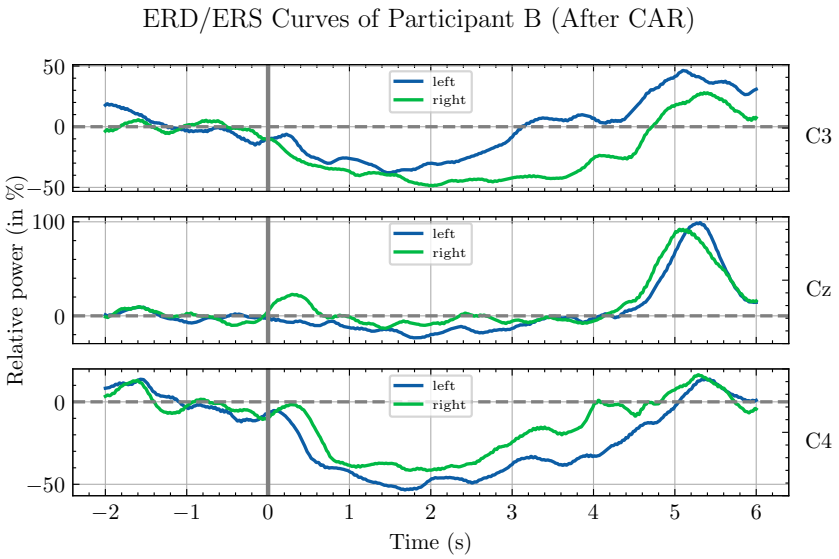

(b)

Figure 5.5: ERD/ERS curves of participant B for different motor imagery tasks. Each subplot shows a different channel on the sensorimotor cortex. It can be seen that a clear cut separation between both classes was not possible as it was for participant E. However, C3 and C4 in (b) show that a separation between both classes was possible for the 2-5 s time period.

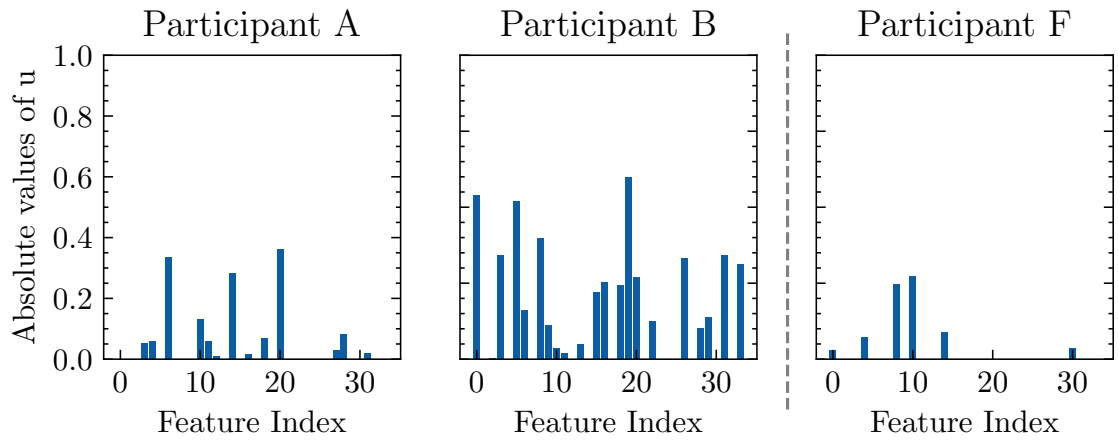

Figure 5.6: Lasso coefficients of SFBCSP for the BCI Competition IV-1 data set. Participants that achieved the best performance boost from SFBCSP are plotted on the left side of the dashed line, whereas the participant with a drop in accuracy was plotted on the right. It can be seen that for the participants with good performance, the feature vector is rather non-sparse. Although SFBCSP looks for sparse feature vectors, the current implementation seems to be working better for less sparse feature vectors.

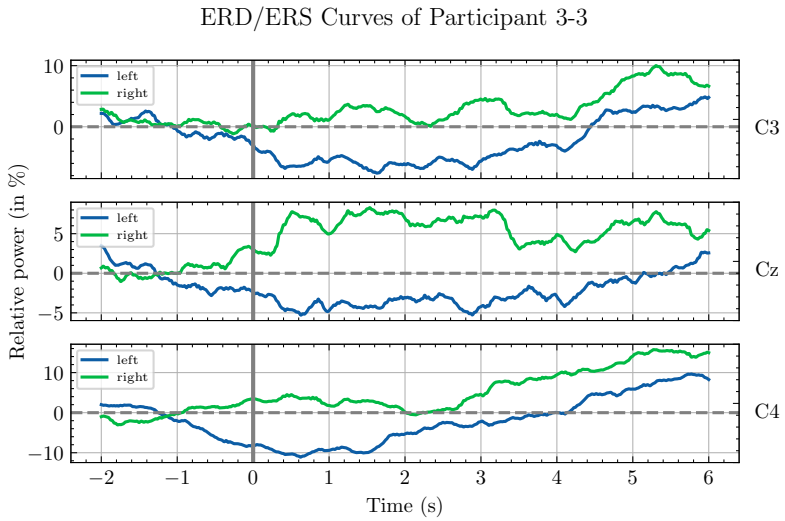

(a)

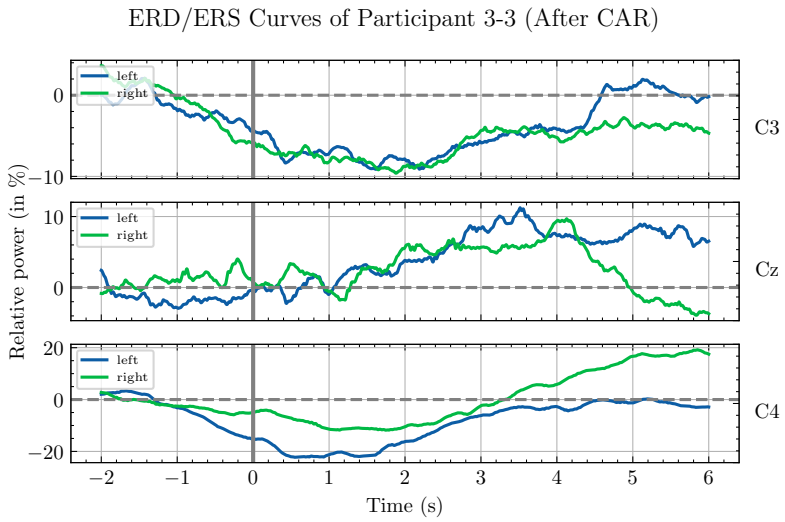

(b)

Figure 5.7: ERD/ERS curves of participant 3 from session 3 for different motor imagery tasks. Each subplot shows a different channel on the sensorimotor cortex. It can be seen that a clear cut separation between both classes was not possible. The only result in line with the expectations came from C4 in (b). There was a clear left hand MI related ERD between -1 and 2 s.

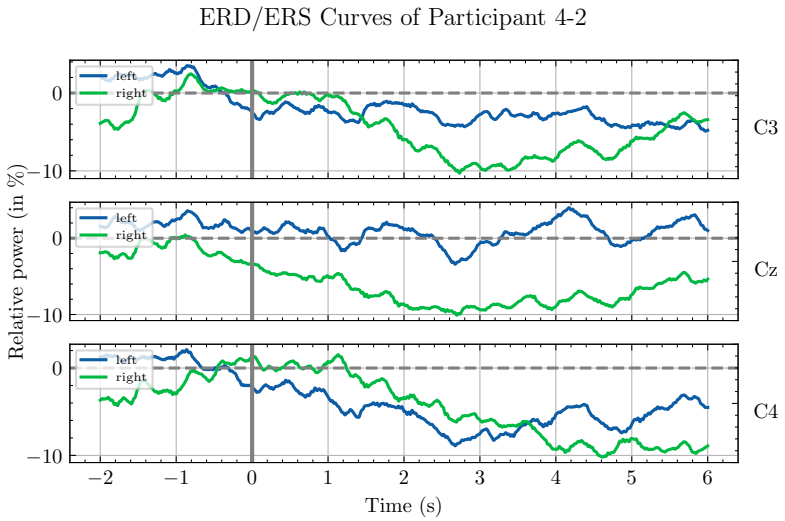

(a)

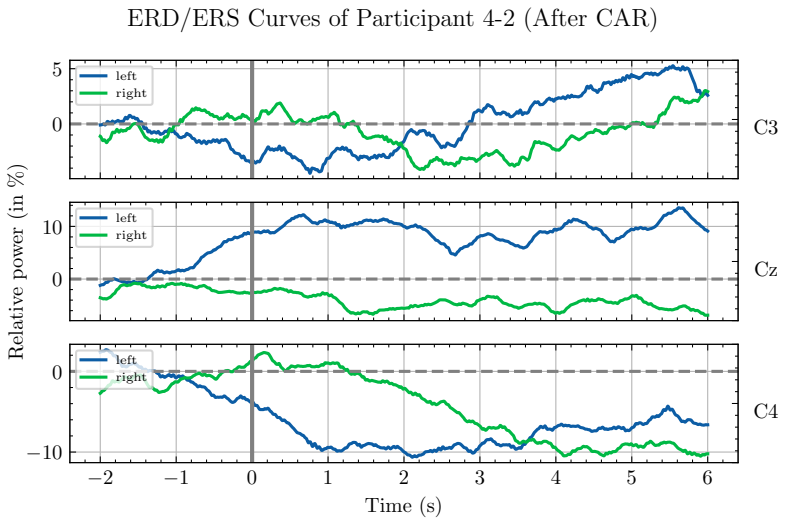

(b)

Figure 5.8: ERD/ERS curves of participant 4 from session 2 for different motor imagery tasks. Each subplot shows a different channel on the sensorimotor cortex. It can be seen that the signals for different MI tasks could be theoretically separable by using Cz with either C3 or C4. However it is very difficult to come up with a neurophysiological explanation of the data.

6 Discussion

This study dealt with building an EEG-based eye blink detection system with multiple control signals, and the investigation whether this system could be used to extend a MI-BCI using the Unicorn Hybrid Black. For the investigation of MI integration, first the results of a publicly available data set (BCI Competition IV-1) were used. These results showed that a combination of ERD/ERS curves, CSP and SFBCSP were very helpful for classifying MI data. The same methods were then applied to the data set recorded with the Unicorn Hybrid Black. The results showed that it was not possible to reproduce the good classification results between different MI classes as it was the case for the publicly available data set.

Bearing the results from chapter 5 in mind, in this chapter the scientific questions posed in chapter 1 will be addressed one by one.

1. *Can single eye blinks be detected using a single EEG channel? How does this system perform?*

It was shown that single eye blinks could be detected with a very high accuracy and that the false detection rates were very low. The RTs for all conditions were around 1 s. All these were achieved by using the activity of only one frontal channel.

These results meant that single eye blinks could be reliably detected in real-time using a single EEG channel.

2. *Can double eye blinks be detected using a single EEG channel? How does this system perform?*

After the eye blink detection system was extended to support a second control signal, namely double blinking, the system was tested again using the same evaluation methods used for the single blink detection case. RTs increased slighty compared to the single blink detection case. This was because of the need to implement a waiting period for a double blink to occur.

The RTs were under 2 s for both of the participants. Given that the participant specific parameters were correctly set, the detection accuracies for both single and double blink detections were above 75%.

In this case, the false detection rates were minimized to 0% for all rest periods. This meant that the system would not act without voluntary input, i.e. blinks, from the user. An even better estimate for this phenomenon came from the pause periods.

Until after the experiment was over, participants were not aware that their signals from the pause periods would also be used to estimate false detection rates. This way

they would not restrict themselves to be as still as possible like for the rest periods. And that is why pause periods gave a better estimate to how the system would perform in a real-life scenario. The false detection rates for these pauses were less than 5%.

Except for one condition, the correct detection accuracies of single blink detections were slightly higher than double blink detections. This verified the assumption that producing double blinks that would get detected by the system was more difficult than producing single blinks. Nevertheless, all these results showed that the system could be reliably used with both single and double voluntary blinks.

One last thing to mention is that, it was shown that only one channel was enough for this eye blink detection system. This meant that the whole system can be made even more compact and portable if only this one channel is used. This can be theoretically possible by disassembling a relatively low-cost EEG system. An example of such a system can be seen in Figure 6.1.

Source: https://www.unicorn-bi.com/product/unicorn-naked-bci/

Figure 6.1: Unicorn Naked BCI is an 8-channel EEG amplifier for BCI applications. It comes without a cover, meaning that it could be possible to disassemble it to have only one channel to be used for eye blink detection. This way, the system would be made as compact and portable as possible for real-life applications.

3. *Can the eye blink detection system be reliably used within only one session?*

Both participants demonstrated that they could produce excellent results within only one session. No extensive training or setup was needed to operate the system (although it will be discussed in the next point that there was a learning effect).

Due to these reasons it can be concluded that the proposed system could be reliably used as a first EEG-to-computer interface in order to, e.g., motivate participants in

volunteering for BCI experiments. Seeing that there is a real-life use to the studied systems, participates could be more willing to cooperate during experiments.

4. *Does feedback influence the eye blink detection system?*

Feedback did not have a significant effect on the RTs. But the accuracies got significantly better in the case of CF. In this case, participants could experience a concrete reaction from the system, i.e. vibration of the motor or the blinking of the LED. It can be assumed that this feedback gave them the confidence that they were able to produce the correct control signals for the system.

The increased performance could also be due to a learning effect. One argument could be that since the CF block was in the end of the experiment, participants already familiarized themselves with the system, thus producing better results. In this case, the improved performance of the system would be more about learned skills than the feedback.

It is very difficult to discard this argument. However, the feedback given by participant 1 was valuable for this discussion. Without being explicitly asked or led to provide any feedback, he said that the CF made a huge difference for him. He mentioned that by seeing that his actions would get translated into real life controls, he could better adapt the strength and frequency of his eye blinks. Comparing this with the other feedback conditions he said that he could do this by learning with the help of the feedback. Looking at his accuracy results for the CF condition, it can be seen that this learning effect really played a role in producing better results.

Bearing this finding in mind, if the eye blink detection system was ever to be deployed in real life, it would be worthwhile to provide users with some sort of real control feedback to improve its overall performance.

5. *Can the detected blinks be used as control signals for IoT (Internet of Things) devices?*

It was shown that a basic UDP connection could be used to send detected eye blinks as control signals to an ESP32. This allowed the control of the vibrotactile motor and LED connected to the microcontroller.

This was done as a proof of concept for other types of IoT control. Since it was shown that the eye blink detection system worked reliably on its own, connecting the blink detections with any type of interface is rather a communication problem between different devices.

In future research, the vibrotactile motor of the circuit could be replaced with, for example, the vibrotactile motor of a smartphone. This way a patient with neurological conditions could directly send signals to his/her caretaker's smartphone in case help was needed.

6. *How do offline analysis methods perform on an "ideal" data set?*

A combination of ERD/ERS curves and filtering gave an insight to the data and participant at hand. It was remarkable that just by looking at the ERD/ERS curves of participant E, the participant's high accuracy score could be anticipated.

In cases where the ERD/ERS curves were not as clean as for the participant E, the curves still carried some information. It was demonstrated that better accuracy scores could be achieved by adapting the epoching window to match the most discriminative ERD/ERS region. Doing this for participant B resulted in an accuracy score increase of 17%. It also decreased the performance of participant G from 92% to 48%. This example demonstrated the participant-specific dynamics of EEG data.

The performance of broad-band (4-40 Hz) CSP was then compared with SFBCSP, an alternate approach that automatically finds participant-specific frequency sub-bands to be used as CSP features for optimal performance. The implemented SFBCSP altered slightly from the original work [31] but it still produced a boost in classification accuracy for more than half of the participants. Although the computation time was significantly higher for this approach, the classifier accuracies showed a significant improvement.

All in all, it was possible to classify different MI tasks using the methods investigated in this study.

7. *How do offline analysis methods perform on a data set recorded with the Unicorn Hybrid Black?*

The same methods were applied to a data set recorded with the Unicorn Hybrid Black, an 8-channel wireless EEG system. Unfortunately the results did not look promising. The ERD/ERS curves seemed to have carried only little information and neither CSP nor SFBCSP performed above chance level for any of the recording sessions.

Bearing in mind that it was demonstrated on an ideal data set that the implementation of the used methods were correct, the results can be explained in different ways.

First, the most obvious possible reason was that the data quality was not high enough. It was shown that there was a significant line noise interference in the data. Even though this noise was filtered out, it has to be kept in mind that there is no substitute for clean data [43].

Unicorn Hybrid Black electrodes are very sensitive to noise. When someone does even a tiniest movement close to the electrodes, the signal amplitude grows very large and it takes a few seconds for it to settle again. Even though there was extra care given to keeping the recording chamber free of any interferences, large scraps of data had to be discarded during automatic epoch rejection because they were contaminated with artifacts that could not be cleaned by filtering alone.

Another reason of the poor performance could be the low number of electrodes. Even though it was shown that by using just two electrodes (C3 and C4), a single trial classification accuracy of 80-95% could be achieved after six to ten sessions [51] [52] [32], a large number of electrodes (e.g., 27) may be needed for CSP [34] which was not the case for the Unicorn Hybrid Black with only eight channels.

Keeping in mind that the ERD/ERS curves not looking promising at all, it can be assumed that there were other issues that have to be addressed in future work before

deciding to completely switch the analysis method. These could range from problems during data acquisition to suboptimal preprocessing steps.

Another possibility is that the participants were either BCI-illiterate or that they had not attended enough recording sessions to produce good results. This possibility could be addressed by recording from different participants or also by designing more interactive recording paradigms to keep the participates engaged in the task.

As it can be seen, there are many possibilities why the MI classification did not work as intended. Unfortunately based purely on the results of this study, it cannot be concluded which ones of these were the sources of this issue. However there are many possible branches to explore in future studies.

Summarized, this study could not provide acceptable MI classification performance using the Unicorn Hybrid Black. However, based purely on the findings of this study, it cannot be concluded that this will always be the case.

8. *Can an online MI-BCI be realized with the Unicorn Hybrid Black?*

Since offline analysis of the recorded data set did not produce acceptable results, this question had to be left unanswered in this study. Future research may show that it can be indeed the case that Unicorn Hybrid Black can be used for an online MI-BCI.

9. *Can the eye blink detection system be extended to support MI?*

Although a MI-BCI could not be built using the Unicorn Hybrid Black, this question can be addressed in a different way. As briefly discussed before, the eye blink detection system can be used not only to allow more degrees of freedom to an MI-BCI, but also to motivate participants. Both participants that attended the MI data recording part of this study made it very clear that they stopped enjoying the recording session directly after the first session. This was both because of the mental work required to sit through the whole experiment, minimizing movements and distractions and also because it was not entertaining to sit through a very long experiment not receiving any feedback.

However, data acquisition is one of the most important steps of building a MI-BCI. This means that keeping the participants engaged in the task is very crucial and that it indirectly aids an MI-BCI. Here, the eye blink detection may come into play.

It is possible to design a recording paradigm where participants have to alternatingly do pure MI in one block and CF eye blink detection in another. This could solve the problem of having to go through a long recording where the participants do not enjoy themselves. It could also potentially increase the connection between voluntary eye blinks and MI in the participant's mind because he/she would be doing these tasks consecutively. This might help with participants getting more familiar with a system that combines these two paradigms. So that if such a system actually gets built, the participants would already have most of the necessary training to operate it.

Of course this idea is rather arbitrary and was proposed more as a fruit for thought. Nevertheless, it might be very a interesting idea for future research.

Summarized, it can be said that the current study could not come up with a lot of findings that would support the hypothesis that an MI-BCI can be aided by an eye blink detection system. This however does not mean that it is totally unfeasible. More future research is needed to study this question in more depth.

7 Conclusion

In this study an eye blink detection system was built using only one frontal EEG channel. This system was evaluated based on it reaction time, detection accuracy and false detection rates. It was shown that this system could support one or two control signals. These control signals were then connected with the ESP32 microcontroller to allow wireless communication with its peripherals. Thus participants could control a vibrotactile motor and an LED within one recording session using their blinks. This was designed as a proof of concept for EEG-based IoT control.

After successfully building the eye blink detection system, the possibility of extending an MI-BCI with it was investigated. This investigation was valuable, as MI-BCI usually takes long training sessions to be used effectively. However, extending an MI-BCI with a system that participants can effectively use within only one session would overcome the need for long waits to operate an EEG based BCI.

For this purpose, the publicly available BCI Competition IV-1 MI data set provided by the Berlin BCI group was used to implement and test different offline analysis methods to classify MI data. First ERD/ERS curves were plotted for different participants to get a sense of the data at hand. This also made it possible to re-examine previous findings like the cortical homunculus and motor imagery coupled brain activities like ERD and ERS. By applying CSP and SFBCSP test set accuracies of above 90% could be achieved.

Then MI data was recorded using a wireless 8-channel dry electrode EEG system following the Graz paradigm. Two participants were recorded for four consecutive days. The offline analysis methods applied to the BCI competition data set were then applied to this recorded data set to see if the Unicorn Hybrid Black EEG system could be used for an MI-BCI.

It was not possible to achieve the same good results on the recorded data set as the ones achieved for the BCI competition data set. This prevented a Unicorn Hybrid Black-based online MI-BCI to be built for this study. That is why it could not be directly studied whether an MI-BCI can be extended with eye blink control signals.

However, the findings could still be used to assess this possibility. It was discussed that by providing the participants with concrete results, like controlling peripherals of a microcontroller with eye blinks detected using EEG, their engagement could be increased. This could be best observed by comparing the moods of the first two participants who attended the eye blink detection experiment with the two other participants who recorded MI data. Clearly the participants who had the feeling that they were in control by using the eye blink detection system were more enthusiastic for attending more experiments. This shows that the sense of agency can help with participants' attentiveness during experiments.

Following this idea further, it was proposed that a recording paradigm could be built that mixes both MI and eye blink detection to keep the participants engaged during recording sessions. This way it could be possible to link the use of eye blink detection and MI-BCI in participants' minds early on during necessary recording sessions. By keeping them engaged in the tasks, better results could be obtained, even when using a dry electrode EEG system with a low number of electrodes, like the Unicorn Hybrid Black. Of course, this is merely a speculation. But the idea is exciting enough to be studied in future research.

To conclude, it can be said that the current study produced valuable results for future research. It showed that voluntary eye blinks detected from a single EEG channel can reliably be used as control outputs within only one session. It further showed that these outputs can be used in a wireless environment to control external devices. It was demonstrated that providing participants with real control feedback achieved better performances while operating a real time system and that there was a learning procedure during this feedback period. Furthermore, it was shown that wireless dry electrode systems may not work as intended out of the box and therefore special care has to be given during recording sessions to acquire good quality data.

Hopefully all these results will be beneficial for future research aiming to combine electrooculography with electroencephalography.

List of Figures

List of Tables

Bibliography

[1] H.-J. Hwang, S. Kim, S. Choi, and C.-H. Im, "EEG-Based Brain-Computer Interfaces: A Thorough Literature Survey," *International Journal of Human-Computer Interaction*, vol. 29, no. 12, pp. 814–826, Dec. 2, 2013, ISSN: 1044-7318, 1532-7590. DOI: 10.1080/10447318.2013.780869.

[2] M. Alimardani, S. Nishio, and H. Ishiguro, "Brain-Computer Interface and Motor Imagery Training: The Role of Visual Feedback and Embodiment," in, Oct. 17, 2018, ISBN: 978-1-78984-069-8. DOI: 10.5772/intechopen.78695.

[3] L. Frolich, I. Winkler, K.-R. Muller, and W. Samek, "Investigating effects of different artefact types on motor imagery BCI," *Annual International Conference of the IEEE Engineering in Medicine and Biology Society. IEEE Engineering in Medicine and Biology Society. Annual International Conference*, vol. 2015, pp. 1942–1945, 2015, ISSN: 2694-0604. DOI: 10.1109/EMBC.2015.7318764. pmid: 26736664.

[4] S. R. Soekadar, M. Witkowski, C. Gómez, E. Opisso, J. Medina, M. Cortese, M. Cempini, M. C. Carrozza, L. G. Cohen, N. Birbaumer, and N. Vitiello, "Hybrid EEG/EOG-based brain/neural hand exoskeleton restores fully independent daily living activities after quadriplegia," *Science Robotics*, vol. 1, no. 1, eaag3296, Dec. 6, 2016, ISSN: 2470-9476. DOI: 10.1126/scirobotics.aag3296.

[5] B. Blankertz, G. Dornhege, M. Krauledat, K.-R. Müller, and G. Curio, "The non-invasive Berlin Brain–Computer Interface: Fast acquisition of effective performance in untrained subjects," *NeuroImage*, vol. 37, no. 2, pp. 539–550, Aug. 15, 2007, ISSN: 1053-8119. DOI: 10.1016/j.neuroimage.2007.01.051.

[6] R. Leeb, F. Lee, C. Keinrath, R. Scherer, H. Bischof, and G. Pfurtscheller, "Brain-Computer Communication: Motivation, Aim, and Impact of Exploring a Virtual Apartment," *IEEE Transactions on Neural Systems and Rehabilitation Engineering*, vol. 15, no. 4, pp. 473–482, Dec. 2007, ISSN: 1558-0210. DOI: 10.1109/TNSRE.2007.906956.

[7] M. Xu, F. He, T.-P. Jung, X. Gu, and D. Ming, "Current Challenges for the Practical Application of Electroencephalography-Based Brain–Computer Interfaces," *Engineering*, Nov. 22, 2021, ISSN: 2095-8099. DOI: 10.1016/j.eng.2021.09.011.

[8] R. P. N. Rao, *Brain-Computer Interfacing: An Introduction*. New York: Cambridge University Press, 2013, 319 pp., ISBN: 978-0-521-76941-9.

[9] P. L. Nunez and R. Srinivasan, *Electric Fields of the Brain: The Neurophysics of EEG*, 2nd ed. New York: Oxford University Press, 2006, 611 pp., ISBN: 978-0-19-505038-7. DOI: 10.1093/acprof:oso/9780195050387.001.0001.

[10] D. J. McFarland, L. M. McCane, S. V. David, and J. R. Wolpaw, "Spatial filter selection for EEG-based communication," *Electroencephalography and Clinical Neurophysiology*, vol. 103, no. 3, pp. 386–394, Sep. 1997, ISSN: 00134694. DOI: 10.1016/S0013-4694(97)00022-2.

[11] J. R. Wolpaw and E. W. Wolpaw, Eds., *Brain-Computer Interfaces: Principles and Practice*. Oxford ; New York: Oxford University Press, 2012, 400 pp., ISBN: 978-0-19-538885-5.

[12] (). Berger: Über das elektroenkephalogramm des menschen - Google Scholar, [Online]. Available: https://scholar.google.com/scholar_lookup?journal=Arch.+Psychiatr.+Nervenkr&title=%C3%9Cber+das+Elektroenkephalogramm+desMenschen&author=H+Berger&volume=87&publication_year=1929&pages=527-570& (visited on 01/15/2022).

[13] H. H. Jasper and H. L. Andrews, "Electroencephalography. III. Normal differentiation of occipital and precentral regions in man," *Archives of Neurology & Psychiatry*, vol. 39, pp. 96–115, 1938, ISSN: 0096-6754. DOI: 10.1001/archneurpsyc.1938.02270010106010.

[14] H. Jasper and W. Penfield, "Electrocorticograms in man: Effect of voluntary movement upon the electrical activity of the precentral gyrus," *Archiv für Psychiatrie und Nervenkrankheiten*, vol. 183, no. 1-2, pp. 163–174, 1949, ISSN: 0003-9373, 1433-8491. DOI: 10.1007/BF01062488.

[15] G. Pfurtscheller and A. Aranibar, "Evaluation of event-related desynchronization (ERD) preceding and following voluntary self-paced movement," *Electroencephalography and Clinical Neurophysiology*, vol. 46, no. 2, pp. 138–146, Feb. 1979, ISSN: 0013-4694. DOI: 10.1016/0013-4694(79)90063-4. pmid: 86421.

[16] G. Pfurtscheller, "Event-related synchronization (ERS): An electrophysiological correlate of cortical areas at rest," *Electroencephalography and Clinical Neurophysiology*, vol. 83, no. 1, pp. 62–69, Jul. 1992, ISSN: 0013-4694. DOI: 10.1016/0013-4694(92)90133-3. pmid: 1376667.

[17] K. J. Miller, G. Schalk, E. E. Fetz, M. den Nijs, J. G. Ojemann, and R. P. N. Rao, "Cortical activity during motor execution, motor imagery, and imagery-based online feedback," *Proceedings of the National Academy of Sciences*, vol. 107, no. 9, pp. 4430–4435, Mar. 2, 2010, ISSN: 0027-8424, 1091-6490. DOI: 10.1073/pnas.0913697107. pmid: 20160084.

[18] B. Blankertz, R. Tomioka, S. Lemm, M. Kawanabe, and K.-r. Muller, "Optimizing Spatial filters for Robust EEG Single-Trial Analysis," *IEEE Signal Processing Magazine*, vol. 25, no. 1, pp. 41–56, 2008, ISSN: 1558-0792. DOI: 10.1109/MSP.2008.4408441.

[19] J. Kalcher and G. Pfurtscheller, "Discrimination between phase-locked and non-phase-locked event-related EEG activity," *Electroencephalography and Clinical Neurophysiology*, vol. 94, no. 5, pp. 381–384, May 1995, ISSN: 00134694. DOI: 10.1016/0013-4694(95)00040-6.

[20] G. Pfurtscheller and F. Lopes da Silva, "Event-related EEG/MEG synchronization and desynchronization: Basic principles," *Clinical Neurophysiology*, vol. 110, no. 11, pp. 1842–1857, Nov. 1999, ISSN: 13882457. DOI: 10.1016/S1388-2457(99)00141-8.

[21] G. Pfurtscheller, C. Neuper, C. Guger, W. Harkam, H. Ramoser, A. Schlogl, B. Obermaier, and M. Pregenzer, "Current trends in Graz brain-computer interface (BCI) research," *IEEE Transactions on Rehabilitation Engineering*, vol. 8, no. 2, pp. 216–219, Jun. 2000, ISSN: 1558-0024. DOI: 10.1109/86.847821.

[22] F. Cincotti, L. Bianchi, J. del R Millan, J. Mourino, S. Salinari, M. Marciani, and F. Babiloni, "Brain computer interface: The use of low resolution surface Laplacian and linear classifiers for the recognition of imagined hand movements," in *2001 Conference Proceedings of the 23rd Annual International Conference of the IEEE Engineering in Medicine and Biology Society*, vol. 1, Oct. 2001, 655–658 vol.1. DOI: 10.1109/IEMBS.2001.1019020.

[23] H. Ramoser, J. Muller-Gerking, and G. Pfurtscheller, "Optimal spatial filtering of single trial EEG during imagined hand movement," *IEEE Transactions on Rehabilitation Engineering*, vol. 8, no. 4, pp. 441–446, Dec. 2000, ISSN: 1558-0024. DOI: 10.1109/86.895946.

[24] J. Mourino, J. del R Millan, F. Cincotti, S. Chiappa, R. Jane, and F. Babiloni, "Spatial filtering in the training process of a brain computer interface," in *2001 Conference Proceedings of the 23rd Annual International Conference of the IEEE Engineering in Medicine and Biology Society*, vol. 1, Oct. 2001, 639–642 vol.1. DOI: 10.1109/IEMBS.2001.1019016.

[25] D. Lehmann and W. Skrandies, "Spatial analysis of evoked potentials in man—a review," *Progress in Neurobiology*, vol. 23, no. 3, pp. 227–250, Jan. 1, 1984, ISSN: 0301-0082. DOI: 10.1016/0301-0082(84)90003-0.

[26] N. Padfield, J. Zabalza, H. Zhao, V. Masero, and J. Ren, "EEG-Based Brain-Computer Interfaces Using Motor-Imagery: Techniques and Challenges," *Sensors*, vol. 19, no. 6, p. 1423, Mar. 22, 2019, ISSN: 1424-8220. DOI: 10.3390/s19061423.

[27] M. Grosse-Wentrup and M. Buss, "Multiclass Common Spatial Patterns and Information Theoretic Feature Extraction," *IEEE Transactions on Biomedical Engineering*, vol. 55, no. 8, pp. 1991–2000, Aug. 2008, ISSN: 0018-9294, 1558-2531. DOI: 10.1109/TBME.2008.921154.

[28] K. Fukunaga, *Introduction to Statistical Pattern Recognition*, ser. Electrical Science. New York: Academic Press, 1972, 369 pp., ISBN: 978-0-12-269850-7.

[29] Z. Koles, "The quantitative extraction and topographic mapping of the abnormal components in the clinical EEG," *Electroencephalography and Clinical Neurophysiology*, vol. 79, no. 6, pp. 440–447, Dec. 1991, ISSN: 00134694. DOI: 10.1016/0013-4694(91)90163-X.

[30] J. Mueller-Gerking, G. Pfurtscheller, and H. Flyvbjerg, "Designing optimal spatial filters for single-trial EEG classification in a movement task," *Clinical Neurophysiology*, p. 12, 1999.

[31] Y. Zhang, G. Zhou, J. Jin, X. Wang, and A. Cichocki, "Optimizing spatial patterns with sparse filter bands for motor-imagery based brain–computer interface," *Journal of Neuroscience Methods*, vol. 255, pp. 85–91, Nov. 2015, ISSN: 01650270. DOI: 10.1016/j.jneumeth.2015.08.004.

[32] G. Pfurtscheller, C. Neuper, D. Flotzinger, and M. Pregenzer, "EEG-based discrimination between imagination of right and left hand movement," *Electroencephalography and Clinical Neurophysiology*, vol. 103, no. 6, pp. 642–651, Dec. 1997, ISSN: 00134694. DOI: 10.1016/S0013-4694(97)00080-1.

[33] S.-L. Wu, C.-W. Wu, N. R. Pal, C.-Y. Chen, S.-A. Chen, and C.-T. Lin, "Common Spatial Pattern and Linear Discriminant Analysis for Motor Imagery Classification," in *2013 IEEE Symposium on Computational Intelligence, Cognitive Algorithms, Mind, and Brain (CCMB)*, Apr. 2013, pp. 146–151. DOI: 10.1109/CCMB.2013.6609178.

[34] C. Guger, H. Ramoser, and G. Pfurtscheller, "Real-time EEG analysis with subject-specific spatial patterns for a brain-computer interface (BCI)," *IEEE Transactions on Rehabilitation Engineering*, vol. 8, no. 4, pp. 447–456, Dec. 2000, ISSN: 1558-0024. DOI: 10.1109/86.895947.

[35] G. Sun, J. Hu, and G. Wu, "A novel frequency band selection method for Common Spatial Pattern in Motor Imagery based Brain Computer Interface," in *The 2010 International Joint Conference on Neural Networks (IJCNN)*, Jul. 2010, pp. 1–6. DOI: 10.1109/IJCNN.2010.5596474.

[36] G. Dornhege, B. Blankertz, M. Krauledat, F. Losch, G. Curio, and K.-R. Muller, "Combined Optimization of Spatial and Temporal Filters for Improving Brain-Computer Interfacing," *IEEE Transactions on Biomedical Engineering*, vol. 53, no. 11, pp. 2274–2281, Nov. 2006, ISSN: 1558-2531. DOI: 10.1109/TBME.2006.883649.

[37] Q. Novi, C. Guan, T. H. Dat, and P. Xue, "Sub-band Common Spatial Pattern (SBCSP) for Brain-Computer Interface," in *2007 3rd International IEEE/EMBS Conference on Neural Engineering*, Kohala Coast, HI: IEEE, May 2007, pp. 204–207, ISBN: 978-1-4244-0791-0. DOI: 10.1109/CNE.2007.369647.

[38] R. Tibshirani, "Regression Shrinkage and Selection Via the Lasso," *Journal of the Royal Statistical Society: Series B (Methodological)*, vol. 58, no. 1, pp. 267–288, Jan. 1996, ISSN: 00359246. DOI: 10.1111/j.2517-6161.1996.tb02080.x.

[39] S. Evers, B. Bauer, B. Suhr, I. W. Husstedt, and K. H. Grotemeyer, "Cognitive Processing in Primary Headache: A Study on Event-related Potentials," *Neurology*, vol. 48, no. 1, pp. 108–113, Jan. 1, 1997, ISSN: 0028-3878, 1526-632X. DOI: 10.1212/WNL.48.1.108.

[40] J. Lorenz and B. Bromm, "Event-related potential correlates of interference between cognitive performance and tonic experimental pain," *Psychophysiology*, vol. 34, no. 4, pp. 436–445, Jul. 1997, ISSN: 0048-5772, 1469-8986. DOI: 10.1111/j.1469-8986.1997.tb02387.x.

[41] J. A. Caldwell, B. Prazinko, and J. Caldwell, "Body posture affects electroencephalographic activity and psychomotor vigilance task performance in sleep-deprived subjects," *Clinical Neurophysiology*, vol. 114, no. 1, pp. 23–31, Jan. 2003, ISSN: 13882457. DOI: 10.1016/S1388-2457(02)00283-3.

[42] A. de Cheveigné and I. Nelken, "Filters: When, Why, and How (Not) to Use Them," *Neuron*, vol. 102, no. 2, pp. 280–293, Apr. 2019, ISSN: 08966273. DOI: 10.1016/j.neuron.2019.02.039.

[43] S. J. Luck, *An Introduction to the Event-Related Potential Technique*, Second edition. Cambridge, Massachusetts: The MIT Press, 2014, 406 pp., ISBN: 978-0-262-52585-5.

[44] A. Widmann, E. Schröger, and B. Maess, "Digital filter design for electrophysiological data – a practical approach," *Journal of Neuroscience Methods*, Cutting-Edge EEG Methods, vol. 250, pp. 34–46, Jul. 30, 2015, ISSN: 0165-0270. DOI: 10.1016/j.jneumeth.2014.08.002.

[45] A. Widmann and E. Schröger, "Filter Effects and Filter Artifacts in the Analysis of Electrophysiological Data," *Frontiers in Psychology*, vol. 3, p. 233, Jul. 9, 2012, ISSN: 1664-1078. DOI: 10.3389/fpsyg.2012.00233. pmid: 22787453.

[46] P. Virtanen, R. Gommers, T. E. Oliphant, *et al.*, "SciPy 1.0: Fundamental algorithms for scientific computing in Python," *Nature Methods*, vol. 17, no. 3, pp. 261–272, Mar. 2, 2020, ISSN: 1548-7091, 1548-7105. DOI: 10.1038/s41592-019-0686-2.

[47] A. Gramfort, "MEG and EEG data analysis with MNE-Python," *Frontiers in Neuroscience*, vol. 7, 2013, ISSN: 1662453X. DOI: 10.3389/fnins.2013.00267.

[48] M. A. Fischler and R. C. Bolles, "Random sample consensus: A paradigm for model fitting with applications to image analysis and automated cartography," *Communications of the ACM*, vol. 24, no. 6, pp. 381–395, Jun. 1, 1981, ISSN: 0001-0782. DOI: 10.1145/358669.358692.

[49] N. Bigdely-Shamlo, T. Mullen, C. Kothe, K.-M. Su, and K. A. Robbins, "The PREP pipeline: Standardized preprocessing for large-scale EEG analysis," *Frontiers in Neuroinformatics*, vol. 9, Jun. 18, 2015, ISSN: 1662-5196. DOI: 10.3389/fninf.2015.00016.

[50] M. Jas, D. A. Engemann, Y. Bekhti, F. Raimondo, and A. Gramfort, "Autoreject: Automated artifact rejection for MEG and EEG data," *NeuroImage*, vol. 159, pp. 417–429, Oct. 1, 2017, ISSN: 1053-8119. DOI: 10.1016/j.neuroimage.2017.06.030. pmid: 28645840.

[51] C. Guger, A. Schlogl, C. Neuper, D. Walterspacher, T. Strein, and G. Pfurtscheller, "Rapid prototyping of an EEG-based brain-computer interface (BCI)," *IEEE Transactions on Neural Systems and Rehabilitation Engineering*, vol. 9, no. 1, pp. 49–58, Mar. 2001, ISSN: 1558-0210. DOI: 10.1109/7333.918276.

[52] D. McFarland, L. McCane, and J. Wolpaw, "EEG-based communication and control: Short-term role of feedback," *IEEE Transactions on Rehabilitation Engineering*, vol. 6, no. 1, pp. 7–11, Mar. 1998, ISSN: 1558-0024. DOI: 10.1109/86.662615.